AD NUMBER

AD813396

NEW LIMITATION CHANGE

TO

Approved for public release, distribution unlimited

FROM

Distribution authorized to U.S. Gov't. agencies and their contractors; Critical Technology; MAY 1967. Other requests shall be referred to Naval Air Systems Command, Washington, DC.

AUTHORITY

USNASC ltr, 26 Oct 1971

P-7026

STUDY OF STRESS-CORROSION CRACKING OF ALUMINUM ALLOYS

Final Report

(6 April 1966 to 5 April 1967)

May 1967

By

A. J. Jacobs

Prepared Under Contract NOw 66-0309d

for

Naval Air Systems Command
Department of the Navy

by

Rocketdyne
A Division of North American Aviation, Inc.
Canoga Park, California

R-7026

STUDY OF STRESS-CORROSION CRACKING OF ALUMINUM ALLOYS

Final Report

(6 April 1966 to 5 April 1967)

May 1967

By

A. J. Jacobs

Prepared Under Contract NOw 66-0309d

for

Naval Air Systems Command
Department of the Navy

by

Rocketdyne
A Division of North American Aviation, Inc.
Canoga Park, California

FOREWORD

This report was prepared by the Chemical and Material Sciences organization of the Research Division of Rocketdyne, a Division of North American Aviation, Inc., in compliance with Contract NOw 66-0309d, Naval Air Systems Command, U.S. Navy. The contract monitor was Mr. R. Schmidt.

This report covers the period from 6 April 1966 to 5 April 1967. The contributions of the following personnel are gratefully acknowledged: Professor G. Thomas of the University of California at Berkeley, with whom valuable discussions were held; Dr. W. T. Chandler and Mr. E. D. Weisert of Rocketdyne, who have offered constructive comments on the manuscript; Drs. R. Chang and L. J. Graham of the North American Aviation Science Center, who initiated and performed, respectively, the elasticity computations; Mr. N. J. Hoffman of Rocketdyne, who performed the experimental measurements which supplemented the elasticity computations; Drs. D. O. Thompson and C. R. Heiple of the Science Center, who were responsible for the internal friction measurements; and Miss A. Palyo of Rocketdyne, who prepared the replicas and the photographs of the replicas shown herein.

ABSTRACT

A further clarification of the mechanism of stress-corrosion cracking in 7075 aluminum alloy was obtained, particularly with regard to the role of dislocations in the mechanism and to the relationship between dislocation mobility and susceptibility to stress-corrosion cracking; high dislocation mobility reduces susceptibility. It was demonstrated during stress-corrosion tests on 7075-T73 specimens that had undergone prior plastic deformation, that the introduction of dislocations alone did not lower the dislocation mobility sufficiently to diminish the stress-corrosion resistance. This is in contrast to similar experiments with -T6 specimens, wherein precipitation was induced by similiar deformation and the mobility was reduced sufficiently to lower the stress-corrosion resistance. An important role for immobilized dislocations was also suggested by a theoretical calculation of the stress field around an edge dislocation which neighbors a grain boundary precipitate. This calculation, which was based only on elasticity theory and thus precluded plastic flow, indicated that a large tensile stress, theoretically as high as 250,000 psi, could act normal to the precipitate-matrix interface. When the capacity for plastic flow (i.e., the dislocation mobility) was intentionally reduced by notching a stress-corrosion specimen, a rapid failure could be induced in normally resistant 7075-T73 alloy. Fractographic analysis revealed that this was a true intergranular, stress-corrosion failure, similar in every respect to a stress-corrosion failure in 7075-T6 alloy. A slip-line study of progressively deformed 7075-T6 and -T73 alloys indicated that slip takes place throughout the grain and is not confined to the grain boundary margins, thus leading to the ultimate transgranular, ductile type of fracture that is observed in fractographs. Preliminary internal friction measurements were conducted on 7075 alloy in four heat treat conditions: -T6, -T73, a condition intermediate between -T6 and -T73, and an underaged condition. Similar results were obtained for all four specimens.

Abstract (Continued)

to the grain boundary regions, thus leading to the ultimate transgranular, ductile type of fracture that is observed in fractographs. Preliminary internal friction measurements were conducted on 7075 alloy in four heat treat conditions: -T6, -T73, a condition intermediate between -T6 and -T73, and an underaged condition. Similar results were obtained for all four specimens.

CONTENTS

ILLUSTRATIONS

TABLES

INTRODUCTION

The general objective of this program was to clarify the fundamental mechanism of stress-corrosion cracking of aluminum alloys, so that ultimately it will be possible to improve the best existing combinations of strength and stress-corrosion resistance of these alloys. Prior to the current program, studies at Rocketdyne had shown a correlation between characteristic dislocation structures and susceptibility to stress-corrosion cracking for the 7075 aluminum alloy (Ref. 1). Thus, the specific objective of this program was to define more clearly the role of dislocations in the stress-corrosion cracking of 7075 and similar alloys.

During earlier research involving explosive shock loading and tensile deformation, it became evident that dislocations were associated with the stress rather than with the corrosion aspects of stress-corrosion cracking. First, there were no indications of preferential corrosion at or near dislocation sites. Secondly, there was evidence that the very factors which limit dislocation mobility, e.g., other dislocations and precipitate particles, and which thus could lead to the initiation of cracks, were those which increased the susceptibility to stress-corrosion cracking (Ref. 2).

It was also apparent from the previous effort that stress-corrosion lifetime (t_f) is more sensitive to changes in particle density than it is to changes in dislocation density. For example, a several-orders-of-magnitude increase in dislocation density due to shock loading will cause a decrease in t_f of not more than two-thirds; whereas, a 2000-fold decrease in particle density accompanying the transformation of -T6 to -T73 alloy will effect a 100-fold increase in t_f. Also, there is a very rapid increase in t_f after a critical overaging time has been reached. This critical overaging time may correspond to the transformation from Guinier-Preston (GP) zones to a more stable precipitate phase with an accompanying decrease in particle density. In the tensile deformation experiment, prestressing 7075-T6 alloy in the plastic region of the stress-strain curve shortened the time to

failure. This result was attributed to the additional formation of GP zones stimulated by the increase in dislocation density. The great sensitivity of t_f to changes in particle density suggested a basis for treating 7075 alloy to optimize the combination of yield strength and stress-corrosion resistance; dislocation strengthening (work hardening), without concomitant or subsequent precipitation, was demonstrated to be essential to any such improved thermal-mechanical treatment.

The first manifestation of a possibly important interaction between particles and dislocations appeared during the examination of thin films of 7075-T6 alloy (Ref. 1). It was observed in these films that dislocations often occurred next to large grain boundary precipitates (Fig. 1) that were known to pit in a saline medium. Furthermore, no such observation was made in the case of -T73 alloy thin films. Because stress-corrosion cracks form readily at the base of pits in -T6 but not in -T73 alloys, (Ref. 3), the dislocation/grain boundary precipitate interactions were considered significant from the standpoint of stress-corrosion crack initiation, and a theoretical study was undertaken to determine the stress field around an interacting dislocation. This study is described in the following section of this report. Subsequent sections contain discussions of experimental effort, and a mechanism is proposed, which is based on all the Rocketdyne and other finding to date. The experimental program involved tensile deformation of 7075-T73 alloy and the effect of such deformation on stress-corrosion resistance; the stress-corrosion testing of 7075-T6 and -T73 specimens having a severe restriction imposed on their ductility by means of a mechanical notch; fractographic examination of the notched specimens; a replica study of the development of slip lines in progressively deformed 7075-T6 and -T73 specimens; and preliminary internal friction measurements on variously aged 7075 specimens to detect differences (if any) in dislocation mobility.

Figure 1. Transmission Electron Micrograph of 7075-T6 Specimen Showing Close Association of Dislocations and Grain Boundary Precipitates.

CALCULATION OF THE DISLOCATION STRESS FIELD AT A PRECIPITATE-MATRIX INTERFACE

The elastic interaction between an inclusion and the matrix containing dislocations, and thus the forces and stress fields between them, depend to a large extent on the elastic properties of these materials and the geometry and location of the dislocations. Exact elasticity solutions for the case of a circular inclusion and an edge dislocation have been treated by Dundurs and Mura (Ref. 4), who demonstrated that for certain combinations of material constants, the dislocation possesses a stable equilibrium position in the matrix near the interface and that the interaction is very much affected by the orientation of the Burgers vector with respect to the inclusion.

If 7075 alloy were viewed along a grain boundary, it is possible that a particle of $MgZn_2$ would be visible, presenting a circular cross section as shown in Fig. 2.

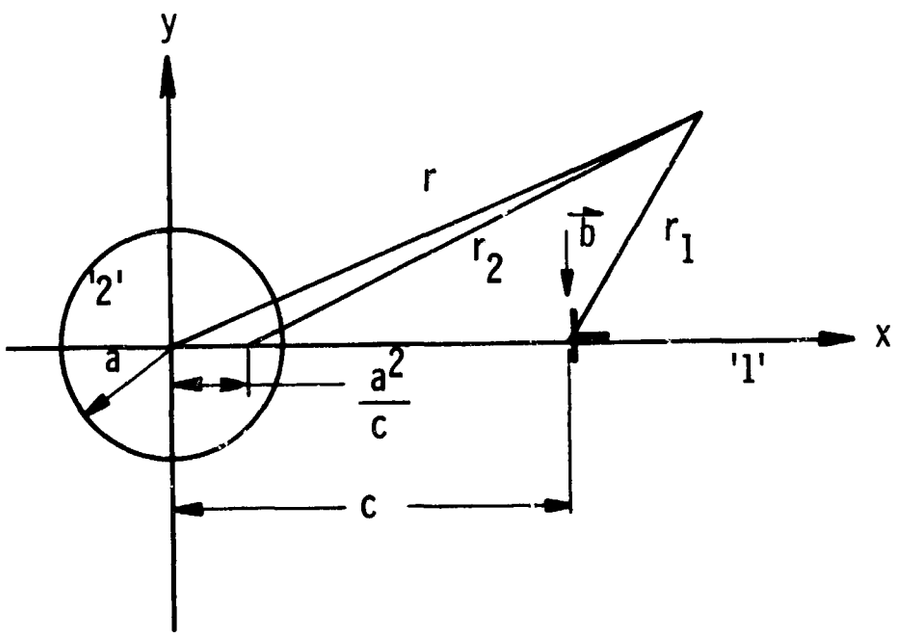

Figure 2. Edge Dislocation in the Neighborhood of a Precipitate Having a Circular Cross Section

A specific example is the case in which an edge dislocation has a Burgers vector in the negative "y" direction. The stress acting normal to the particle-matrix interface is then a special case of the following function:

$$\sigma_{xx} = \frac{G_1 b_y}{\pi (K_1 + 1)} \left\{ -2 \left[1 - \frac{2x_1^2}{r_1^2} \right] \frac{x_1}{r_1^2} + \left[A + B - \frac{4Ax_2^2}{r_2^2} \right] \frac{x_2}{r_2^2} + \right.$$

$$\frac{2A(\beta^2 - 1)}{\beta^3} \left[-\beta^2 + 2\left(\beta^2 - 3 + \frac{4x_2^2}{r_2^2} \right) \frac{x_2^2}{r_2^2} + \right.$$

$$\left. \frac{(\beta^2 - 1)}{\beta} \left(3 - \frac{4x_2^2}{r_2^2} \right) \frac{ax_2}{r_2^2} \right] \frac{a}{r_2^2} - \left[A + B - \frac{4Ax^2}{r^2} \right] \frac{x}{r^2} +$$

$$\frac{\left[A\left(2\beta^2 - 1\right) + M\left(K_2 + 1\right) - 1 \right]}{\beta} \left[\frac{1 - 2x^2}{r^2} \right] \frac{a}{r^2} +$$

$$\left. 2A \left[3 - \frac{4x^2}{r^2} \right] \frac{a^2 x}{r^4} \right\}$$

where

G = shear modulus

Γ = G_2/G_1 ('2' refers to particle and '1' to the matrix)

β = $c/a \geq 1$

γ = Poisson's ratio

K = $3 - 4\gamma$ (for plane strain)

A = $(1 - \Gamma)/(1 + \Gamma K_1)$

B = $(K_2 - \Gamma K_1)/(K_2 + \Gamma)$

M = $\Gamma (K_1 + 1)/(K_2 + \Gamma)\ (K_2 - 1 + 2\Gamma)$

x_1 = $x - c$

x_2 = $x - a^2/c$

An IBM 7094 computer was used to plot the iso-stress contours around the given edge dislocation. The particular plot for the case where G_2/G_1 = 1.2, $\gamma_1 = \gamma_2 = 0.33$, a = 100 b, and c - a = 10 b is shown in Fig. 3. This and similar plots were then used to derive the four curves shown in Fig. 4. The latter curves indicate the variation of σ_{xx} at the particle-matrix interface, with the ratio G_2/G_1, for various distances between the dislocation and the interface.

Preliminary density and dynamic measurements involving the resonant frequency of a cylindrical specimen in torsion have yielded a G_2/G_1 ratio of 2. Referring to Fig. 4, it is seen that for this ratio, σ_{xx} may vary from 12,000 to 250,000 psi as the dislocation-interface distance decreases from 100 to 5 b. These stress values are based on an elastic model and preclude plastic flow in the particle or matrix.

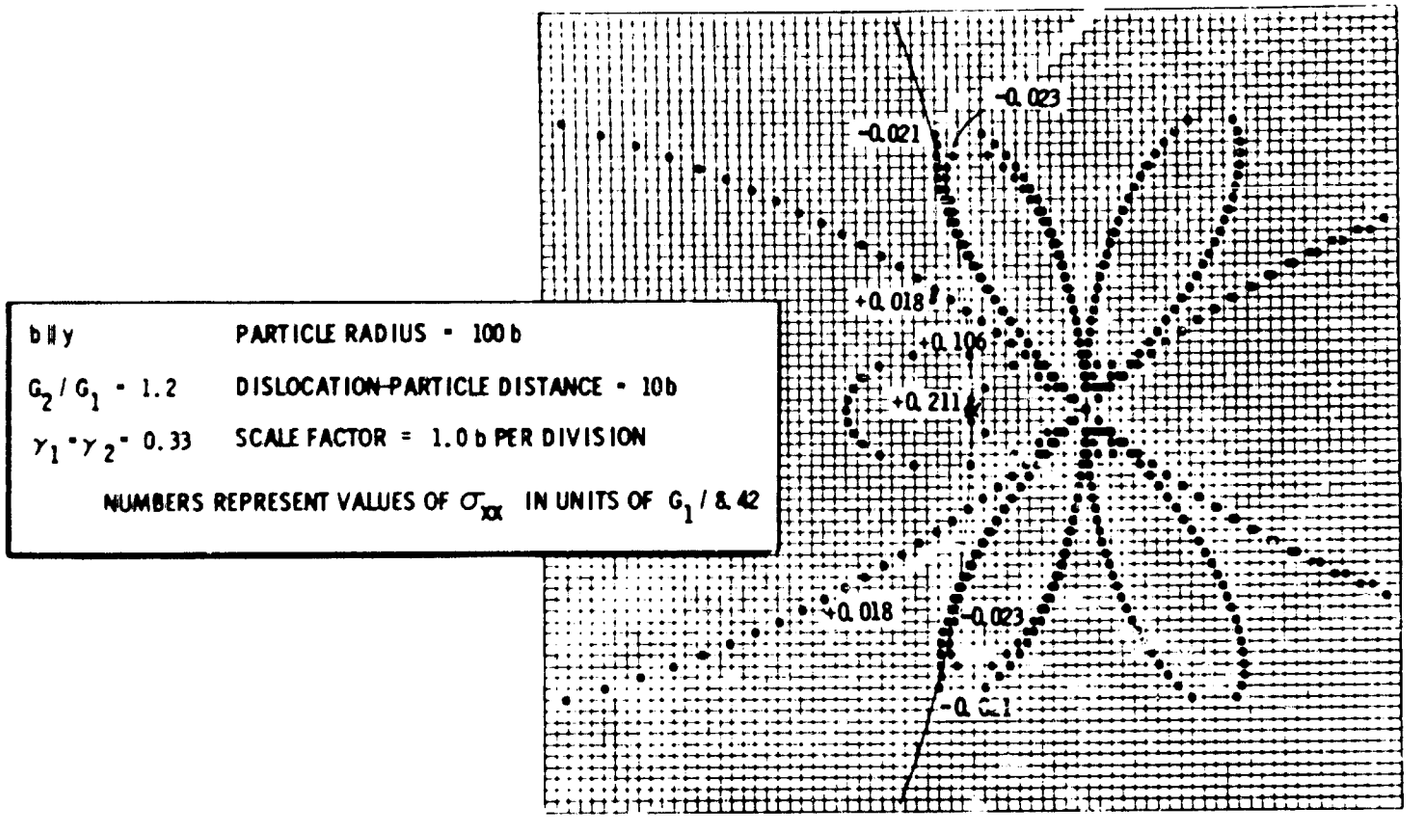

Figure 3. Iso-Stress (σ_{xx}) Contours for an Edge Dislocation Situated Near a Precipitate

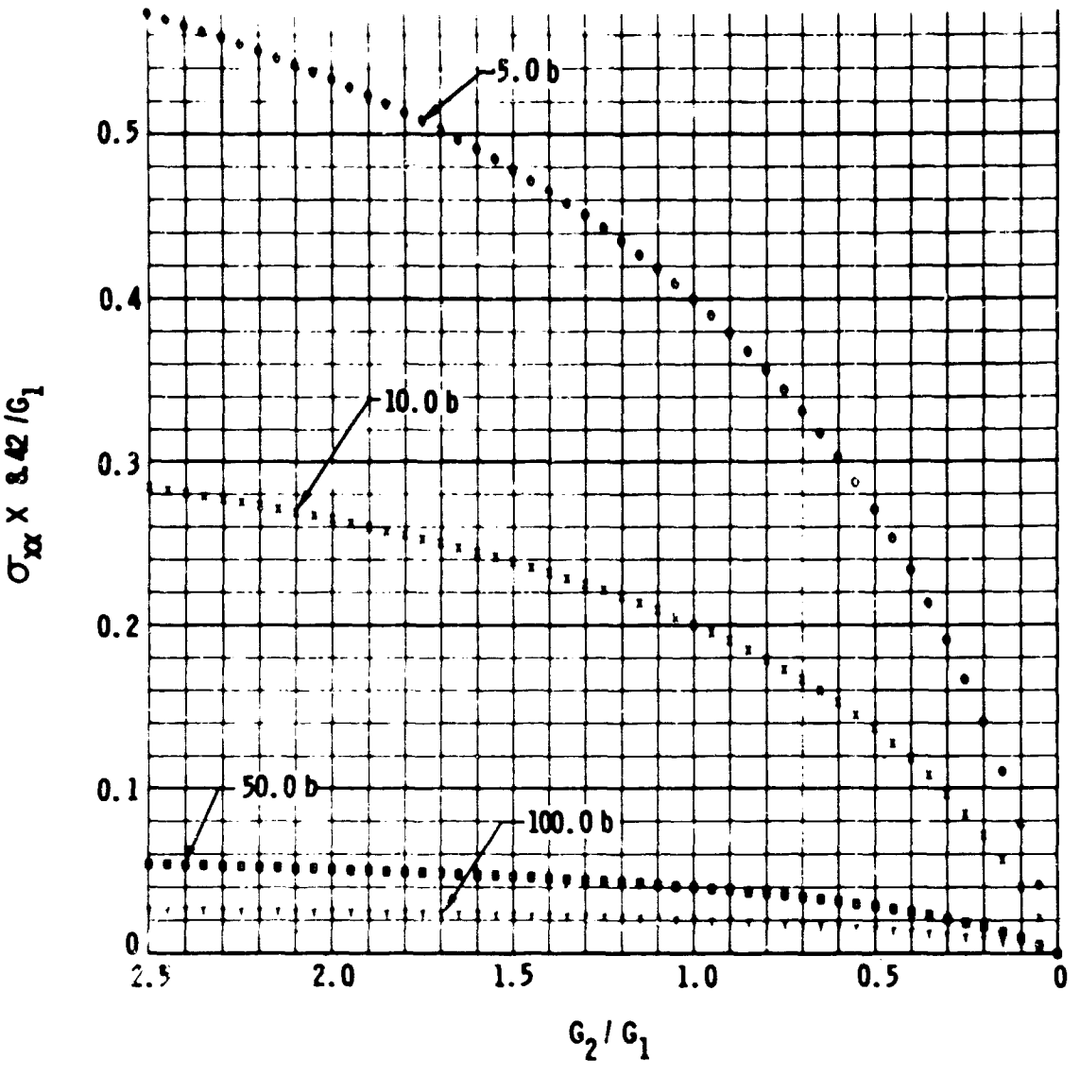

Figure 4. Variation of Tensile Stress at Precipitate-Matrix Interface (σ_{xx}) With Shear-Modulus Ratio (G_2/G_1)

TENSILE DEFORMATION AND THE STRESS-CORROSION RESISTANCE OF 7075-T73 ALLOY

EXPERIMENTAL PROCEDURE

Details of the previous deformation experiment on 7075-T6 alloy have been presented elsewhere (Ref. 2). In general, the experimental procedures used were the same for -T73 and -T6 specimens. However, the specimen design was different and a different stress level was employed.

Four 7075-T73 specimens were subjected to stress-corrosion tests after being plastically deformed in a Universal tensile machine. These tests were of the alternate immersion variety and were conducted in a 3-1/2 percent aqueous NaCl solution. The specimens were loaded in their stress-corrosion frames (Fig. 5) to 75 percent (vs 50 percent in the case of -T6 specimens) of their post-deformation yield strength. The post-deformation yield strengths were measured on a separate group of -T73 specimens, which received the same deformation as the stress-corrosion specimens. There was one important difference between the pre- and post-deformation stress strain curves for the -T6 and the -T73 specimens: the -T6 curves were discontinuous with respect to each other (the post-deformation curves were higher than expected), while the -T73 post-deformation curves merged continuously into the pre-deformation curves as expected (Fig. 6). Part of the increase in yield strength of the -T6 specimens can be attributed to additional precipitation stimulated by the increased density of dislocations. The -T73 tensile and stress-corrosion specimens were 1 8-inch rounds, as shown in Fig. 7 (the -T6 specimens had a flat reduced section, as shown in Fig. 5). The deformation stresses and the post-deformation yield strengths of -T73 and -T6 specimens are presented in Table 1.

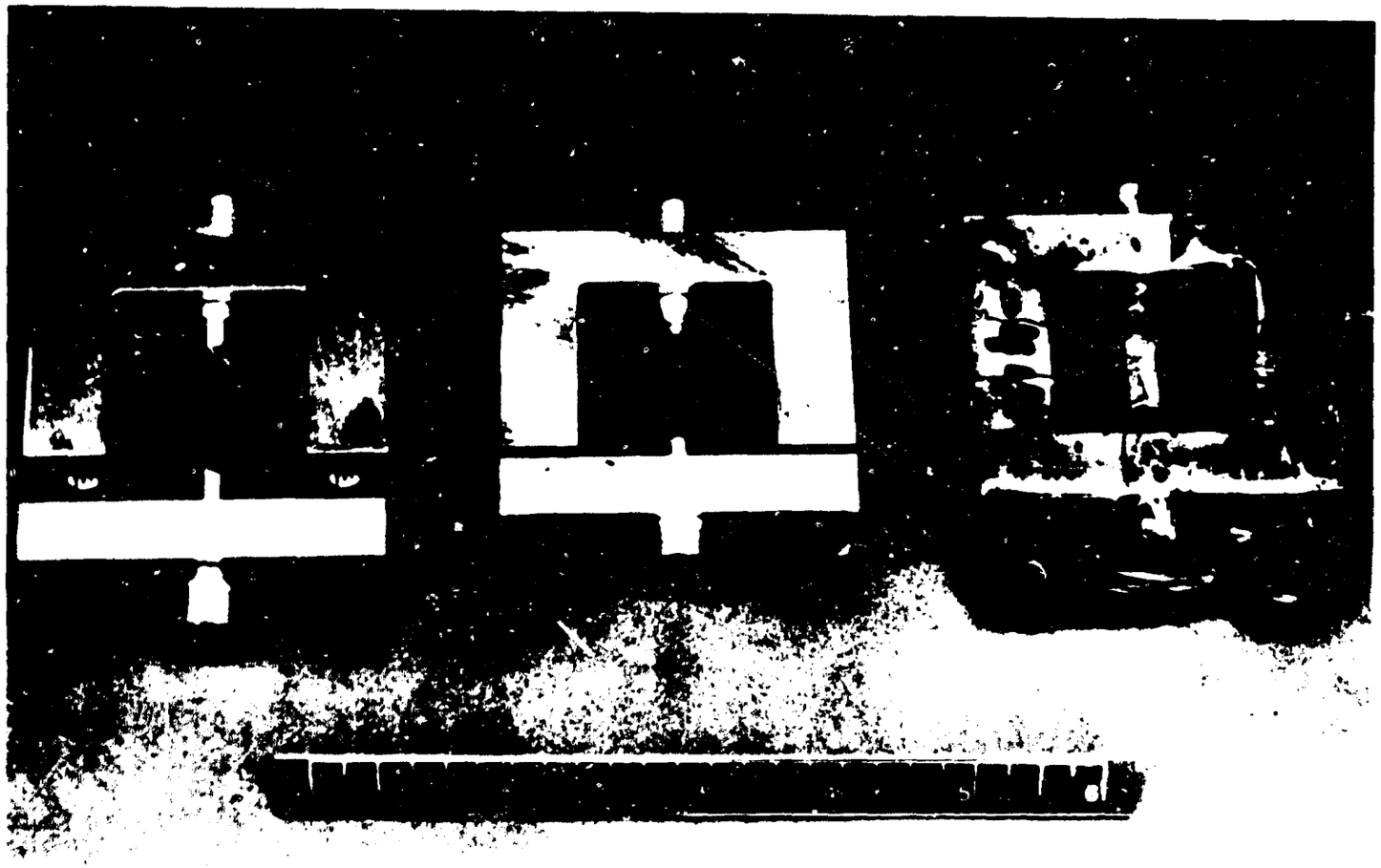

5AJ96-2 4 65-C2B

Figure 5. Assembly of Stress-Corrosion Specimen in Testing Frame

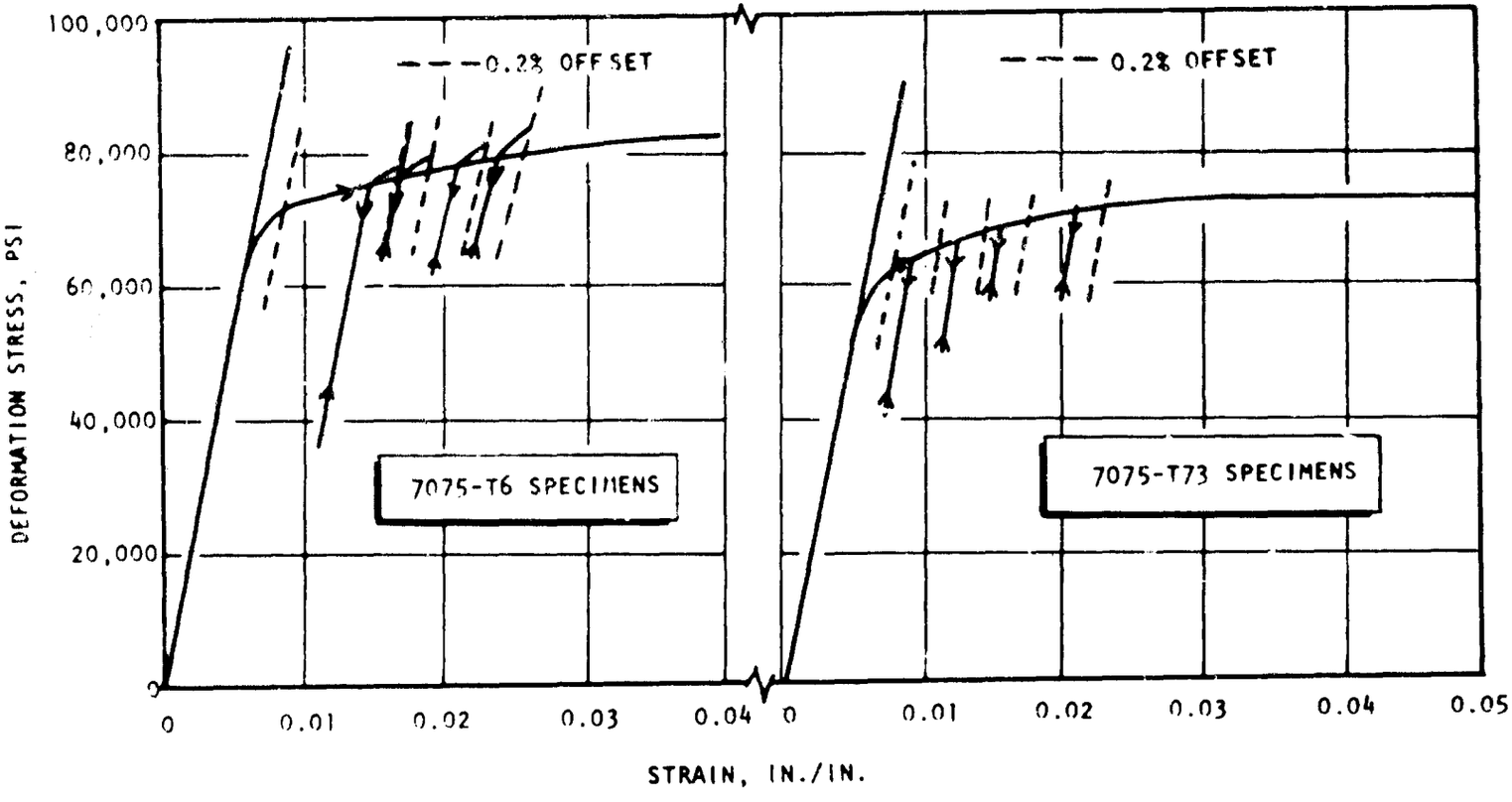

Figure 6. Pre- and Post-Deformation Curves for 7075-T6 and -T73 Specimens

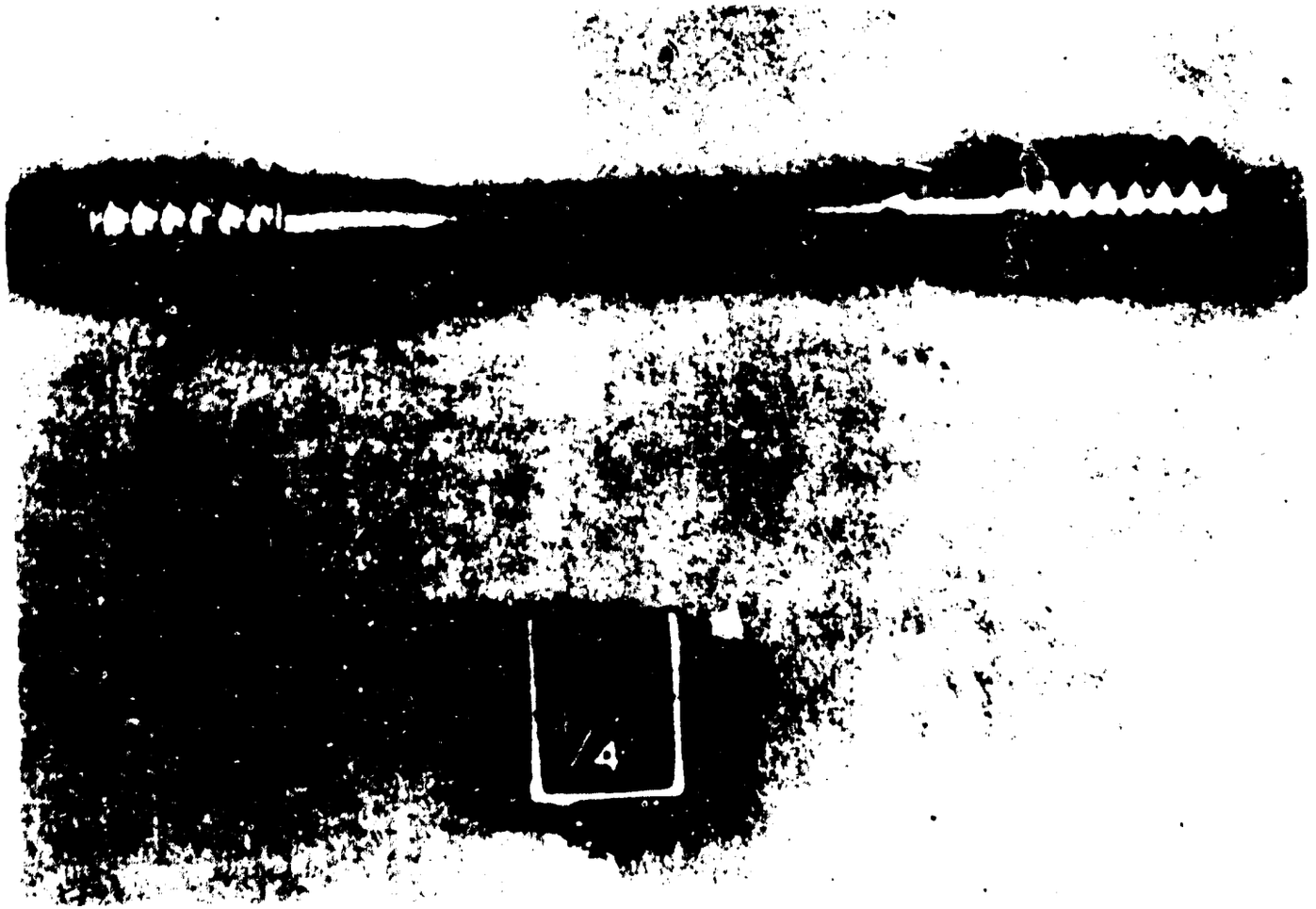

5AJ96-2 4 65-C2A

Figure 7. One-Eighth-Inch Round Stress-Corrosion Specimen

TABLE 1

PRIOR DEFORMATIONS RECEIVED BY 7075-T6 AND
-T73 STRESS-CORROSION SPECIMENS AND
RESULTANT YIELD STRENGTHS

Specimen No.	Deformation Stress, psi	Post Deformation Yield Strength (0.2 percent Offset), psi
7075-T6		
134	75,500	78,100
136	76,800	79,100
139	78,100	81,000
141	79,100	84,300
143 (control)	Undeformed	71,900 (Undeformed)
7075-T73		
8-1	63,000	65,040
5	65,540	67,600
6	67,480	69,550
7-1	69,590	71,700
15, 16, 15-1, 15-2, 15-3, 15-4, 16-1 (Controls)	Undeformed	62,500 (Undeformed)

RESULTS AND DISCUSSION

The stress-corrosion results for the plastically deformed -T6 and -T73 specimens are plotted together for comparison in Fig. 8.

The -T6 curve shows that as the deformation stress is raised from 75,500 to 79,100 psi, the stress-corrosion test life is lowered by more than two-thirds (the t_f of the undeformed control specimen was 7 days). The -T73 specimens, however, were not adversely affected by the prior deformation (Fig. 8). The t_f values varied irregularly between a low of 24 days, at a prestress level of 63,000 psi, and a high of 65 days, at a prestress of 69,590 psi. On the average, these t_f values were greater than the average t_f of seven undeformed controls (26 days; points plotted for load/fracture load = 0.65, Fig. 11).

The preceding results can be explained in terms of dislocation-precipitate interactions. In the -T6 specimens, two factors contributed to the increase in yield strength, first, the increase in dislocation density and second, the increase in particle density resulting from the increase in dislocation density. In the -T73 specimens, however, only the first of these factors was present. Assuming that the increase in dislocation density was not exactly the same in the two tempers, the small difference would easily be overwhelmed by even a small difference in particle density which is now known to be a more important variable than the dislocation density in determining stress-corrosion life. The increase in particle density with increasing prior deformation of -T6 specimens resulted in the progressively shorter time to failure. The accompanying increase in dislocation density in -T6 specimens, or the increase in dislocation density alone in -T73 specimens had a negligible effect on t_f.

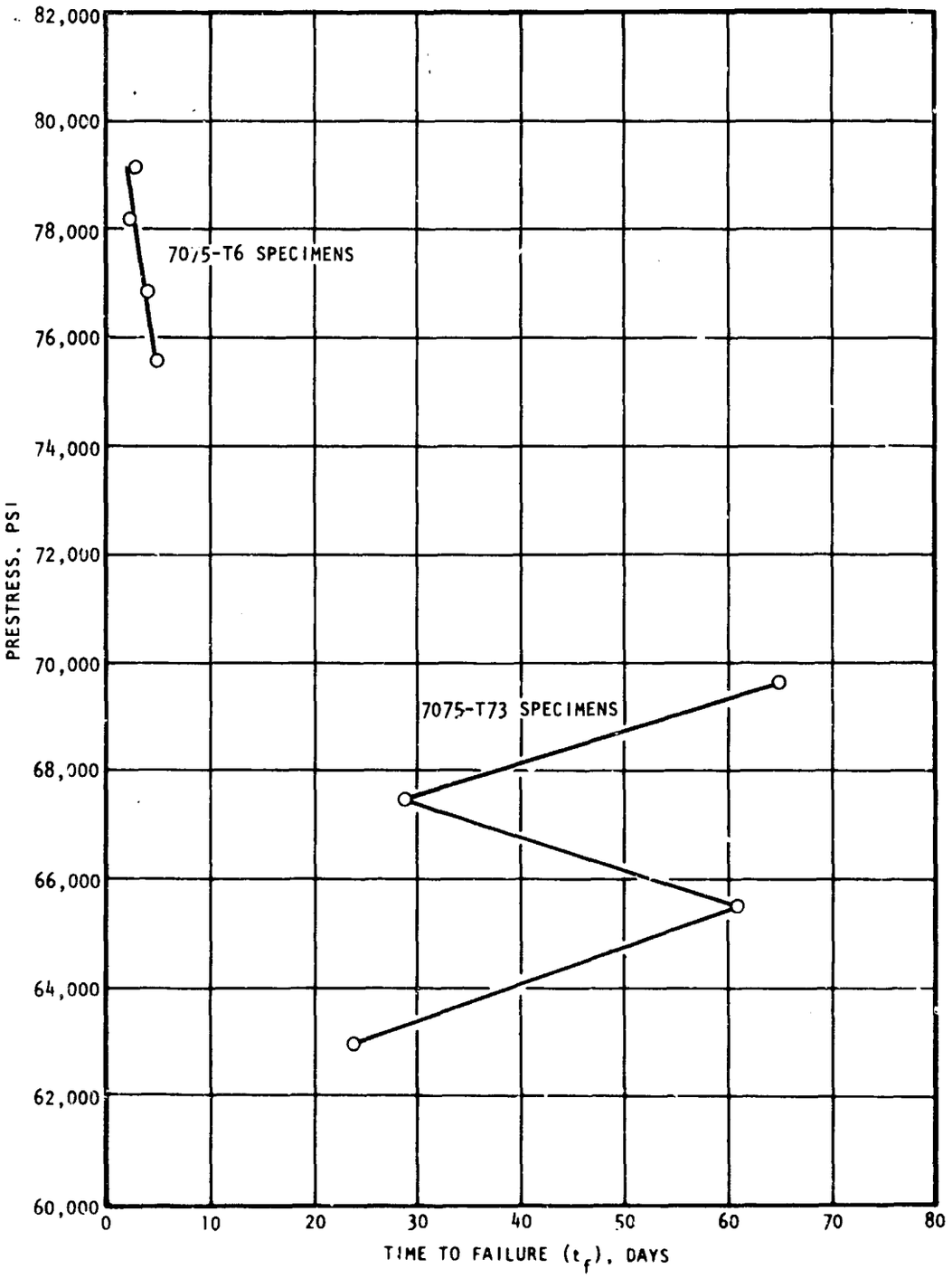

Figure 8. Deformation Prestress vs Time to Failure (t_f) of 7075-T6 and -T73 Specimens

THE LOAD DEPENDENCE OF STRESS-CORROSION LIFETIME OF NOTCHED AND UNNOTCHED 7075-T6 AND -T73 SPECIMENS

The shock loading and tensile deformation experiments, which have been previously described, suggested that the most important difference between the -T6 and -T73 tempers involves the mobility of dislocations and therefore the ease with which plastic flow takes place. The fine dispersion of GP zones in the 7075-T6 temper reduces dislocation mobility and renders plastic flow at the tip of a crack very difficult. Dislocations in the -T73 temper are more mobile because of the coarser particle dispersion, and plastic flow can occur more easily, thus preventing high stress concentrations. It was decided to test these concepts by conducting stress-corrosion tests on notched -T73 specimens. Plastic flow in a notched specimen is localized to the material immediately at the root of the notch. Thus, a notched -T73 specimen should approach, in its behavior, normal -T6 temper behavior in which high stress concentrations can develop at the root of a crack because of restricted plastic flow. In the experiment described in the following paragraphs, stress-corrosion tests were also conducted on notched -T6 and unnotched -T6 and -T73 specimens.

EXPERIMENTAL PROCEDURE

Four 7075-T73 and four -T6 1/8-inch round stress-corrosion specimens were notched, as shown in Fig. 9 , prior to testing. The stress concentation at the root of such a notch is approximately 3.2 (Ref. 5). Eleven unnotched -T73 and five unnotched -T6 specimens served as controls.

The specimens were loaded in stress-corrosion frames to various fractions of the ultimate load. The ultimate loads were determined during tensile tests on separate specimens of the same dimensions and from the same billet as the stress-corrosion specimens. Two tensile tests were conducted for each condition (notched -T73, etc.); typical load-strain curves obtained

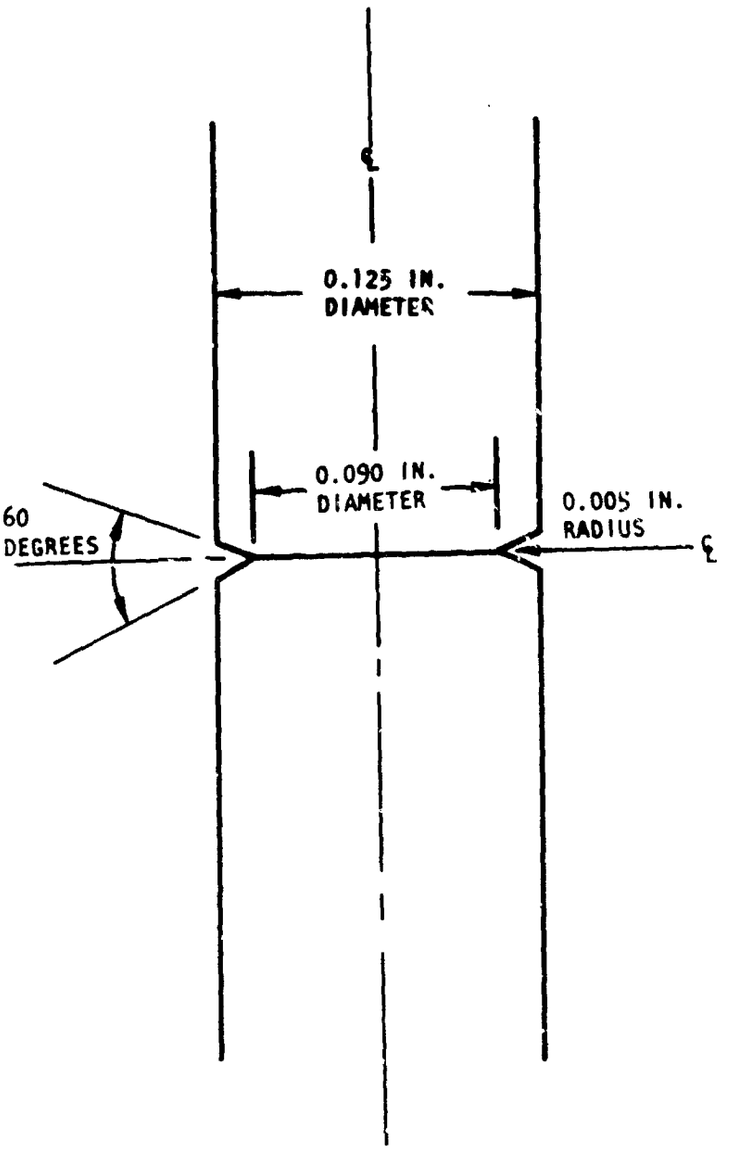

Figure 9 . Notched 1/8-Inch Round Stress-Corrosion Specimen

during these tests are shown in Fig. 10. Each stress-corrosion specimen was strained a preselected amount. The strain was measured by a 1/2-inch extensometer and read on the strain recorder of a Riehle tensile testing machine. The two loads corresponding to this strain in the corresponding pair of tensile tests were averaged, and the average load was divided by the average ultimate load obtained in the same pair of tensile tests. The fractions of ultimate load so computed are presented in Table 2. The region of the load-strain curve (elastic or plastic), to which the load applies, is also indicated in Table 2.

RESULTS AND DISCUSSION

A comparison of results for notched and unnotched -T6 and -T73 stress-corrosion specimens is presented in Fig. 11, where the fraction of ultimate load (P/P_u) applied in the test is plotted against time to failure (t_f). The results indicate that notched -T73 specimens approach the -T6 condition (notched or unnotched), in stress corrosion susceptibility, particularly at high values of P/P_u (>0.9). In fact, the t_f values of the three most highly stressed notched -T73 specimens fall well within the scatter band for unnotched -T6 specimens taken from Ref. 6. A critical P/P_u is suggested for notched -T73 specimens; this is similar to the critical stress for unnotched -T6 specimens (the stress below which stress-corrosion failure will not occur).

The lifetimes of notched -T6 specimens (unlike those of notched -T73) are independent of load. All the notched -T6 specimens failed in 1 day or less as the load varied from 0.27 to 0.95 of the load at fracture. Because unnotched -T6 specimens are known to show a marked dependence on stress (Ref. 6), the effect of the notch is the same in -T6 as it is in -T73 specimens, viz., to enhance the susceptibility to cracking. This enhancement is less dramatic in the case of the -T6 temper, however.

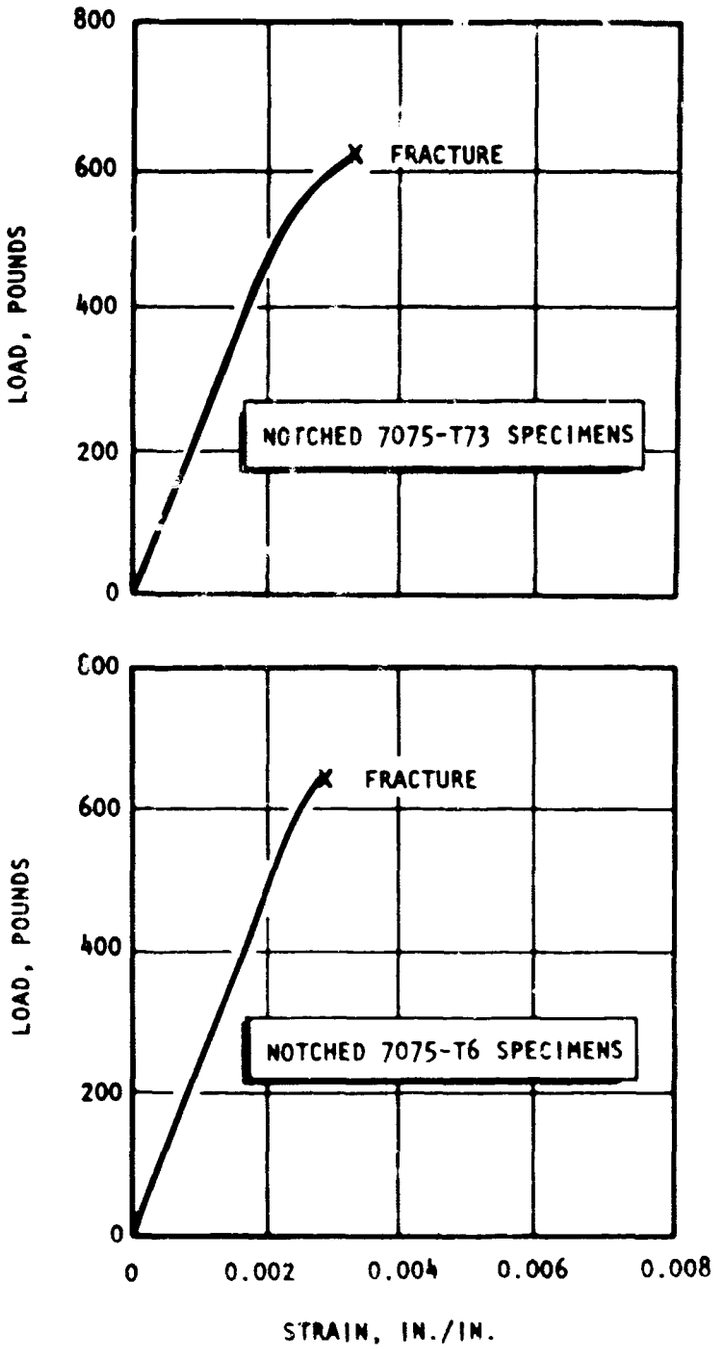

Figure 10. Typical Load vs Strain Curves for Notched 7075-T6 and -T73 Specimens

TABLE 2

FRACTIONS OF ULTIMATE LOAD AT WHICH NOTCHED AND UNNOTCHED 7075-T73 AND -T6 STRESS-CORROSION SPECIMENS WERE TESTED

Condition	Specimen No.	Applicable Region of Load-Strain Curve	Fraction of Ultimate Load	Fractograph
7075-T73				
Notched	17	Plastic	0.79	-
	18	Plastic	0.89	Yes
	19	Plastic	0.95	Yes
	20	Plastic	0.99	Yes
Unnotched	15	Elastic	0.65	Yes
	16	Elastic	0.65	-
	15-1	Elastic	0.65	-
	16-1	Elastic	0.65	Yes
	15-2	Elastic	0.65	-
	15-3	Elastic	0.65	-
	15-4	Elastic	0.65	-
	9-1	Plastic	0.79	-
	10-1	Plastic	0.89	-
	11	Plastic	0.91	-
	12	Plastic	0.98	-
7075-T6				
Notched	27	Elastic	0.27	-
	28	Elastic	0.55	-
	29	Plastic	0.91	Yes
	30	Plastic	0.95	Yes
Unnotched	25	Elastic	0.22	-
	31	Plastic	0.76	-
	32	Plastic	0.84	-
	33	Plastic	0.91	-
	34	Plastic	0.95	Yes

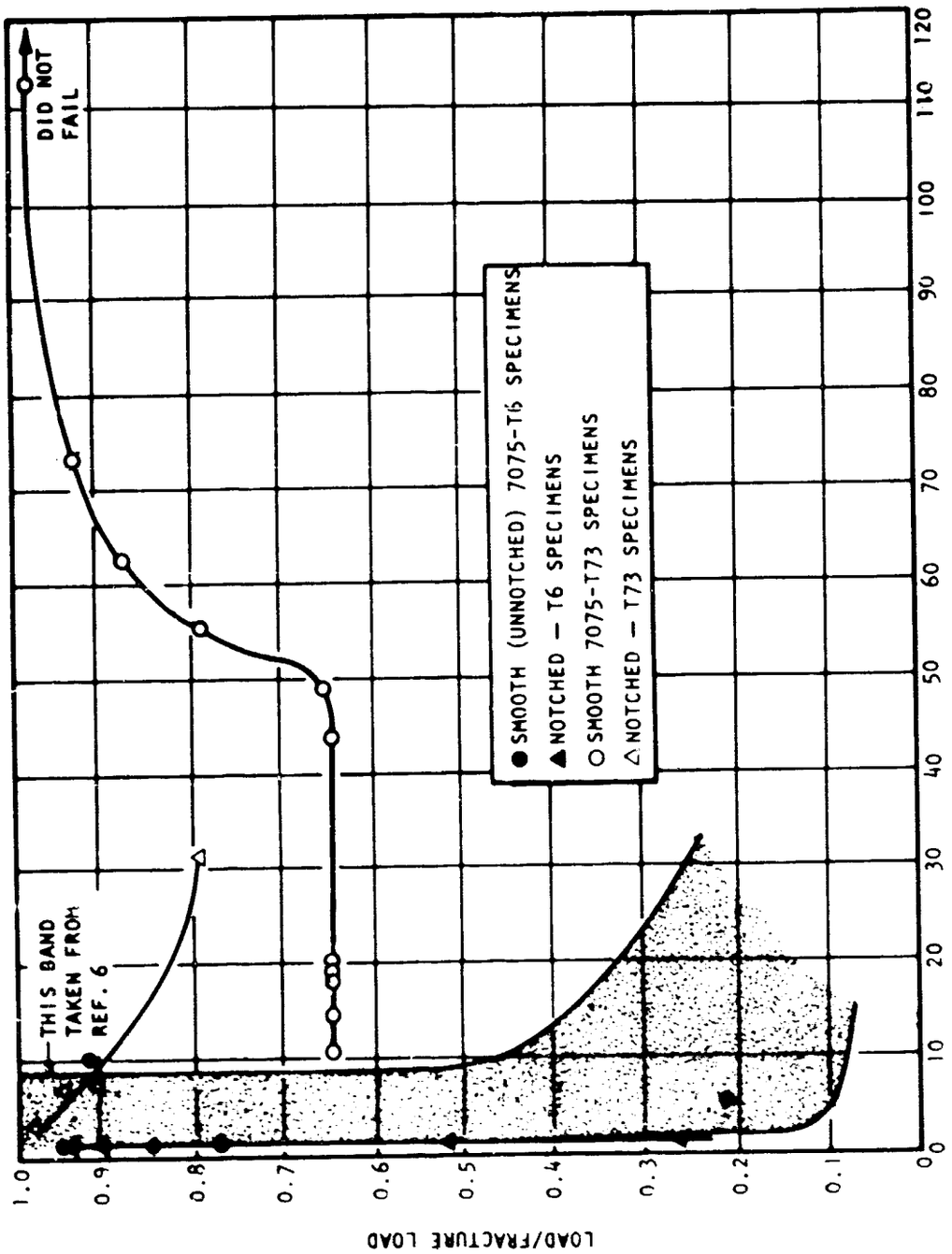

Figure 11. Fraction of Load to Fracture (P/P_u) vs Time to Failure (t_f) of Notched and Unnotched 7075-T6 and -T73 Specimens

The results for the unnotched -T73 specimens are rather surprising. The t_f actually increases with increasing stress level. Although the particular billet from which the specimens were prepared met tensile and conductivity specifications for -T73 material, t_f varied from 10 days to 49 days for seven specimens stressed at 65 percent of their ultimate tensile strength (UTS). Specimens stressed at 79, 89, and 91 percent of their UTS failed in 55, 63, and 74 days, respectively. The specimen stressed at the highest level (98 percent of UTS) did not fail after 112 days of testing.

It is possible that a notch serves to concentrate anodic activity because of the high stresses developed at its root. Such an "area" effect has been observed by Farmery and Evans (Ref. 7) and by Colner and Francis (Ref. 8). Farmery and Evans demonstrated that the stress-corrosion life of a partially coated Al-7 percent Mg specimen increased as the exposed (uncoated) area was reduced. However, when a stressed specimen having a small exposed area was electrically coupled to an unstressed specimen having a large exposed area, the life of the stressed specimen was reduced. This is an electrochemical effect in which the stressed specimen acts as the anode and the unstressed specimen as the cathode, and the magnitude of the current flowing in the differential stress cell increases with increasing stress. Colner and Francis (Ref. 8) have shown that a similar effect operates in the cracking of Al-4 percent Cu alloys. In the present investigation, however, evidence against an area effect was obtained from the notched -T6 specimen (Specimen No. 29) which broke at some distance from the notch. Because the maximum stress requirement for propagation of the crack was obviously met along the path that the crack followed, this path must have been more favorable from a chemical or electrochemical standpoint than any alternative path emerging from the notch.

The different stress dependence of t_f for unnotched -T6 and -T73 specimens (Fig. 11) is attributed to the basic difference between these two tempers in their ability to deform plastically. The differences between

the t_f values of -T6 and -T73 tempers is accentuated as the stress level increases, which suggests that the ratio of maximum stresses present at the root of an advancing crack, $(\text{tensile stress})_{max}/(\text{shear stress})_{max}$ is increasing with applied stress in the case of -T6 and decreasing in the case of -T73 specimens. Thus, at the root of the crack, the stress state is approaching balanced triaxiality in -T6 but deviating more and more from such a condition in -T73 specimens. Any corrosion fissures in -T73 specimens are repeatedly blunted because of the high deformability of this temper.

FRACTOGRAPHY OF NOTCHED AND UNNOTCHED 7C75-T6 AND -T73 STRESS-CORROSION AND TENSILE SPECIMENS

EXPERIMENTAL PROCEDURE

Electron fractographs were prepared from representative fracture surfaces among the notched and unnotched 7075-T6 and -T73 stress-corrosion and tensile specimens. The replicated specimens have been noted in Table 2. The fractured tensile Specimens No. 11-1 (unnotched -T73), 14 (notched -T73), 21 (unnotched -T6), and 23 (notched -T6) were replicated for control purposes. Replicas were of the two-stage plastic-carbon variety and were shadowed with uranium oxide.

RESULTS AND DISCUSSION

The fracture surfaces of the tested stress-corrosion specimens displayed a dark, crescent-like area around the outside and a light area occupying the remainder of the surface. In those cases where the failure was in the notch, the light area was larger; in the other cases, where the failure was away from the notch (Specimen No. 29), or where the specimen had no notch, the dark area was larger. From all indications, the dark area represents a slow, stress-corrosion phase of failure, and the light area a more rapid, tensile-type fracture. The fact that the light area was larger in those specimens where failure was in the notch, as compared to the specimens where failure was away from the notch, is indicative of a much smaller stress-absorbing capacity in the former group of specimens before rapid tensile failure.

The fractographs showed that the fracture surfaces in the dark areas were almost entirely intergranular in nature, while those in the light areas were predominantly transgranular (Fig. 12). Quite severe corrosion had taken place in the dark areas, and the products of the corrosion reaction were considerably more abundant in these areas than in the light areas.

Figure 12a. Intergranular Fracture Typical of Stress-Corrosion Phase of Failure in a Notched 7075-T73 Specimen. (Note corrosion product in rough-textured area.)

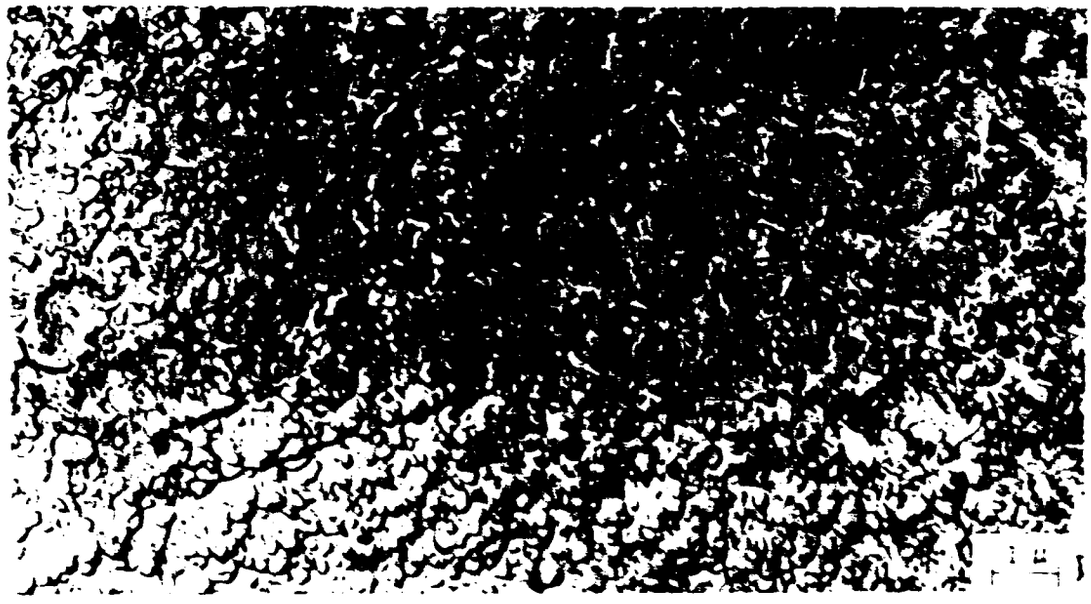

Figure 12b. Fractograph of a Notched 7075-T6 Specimen That Failed Away From the Notch. (Note transgranular fracture typical of tensile phase of failure.)

as might be expected from the relative times that these areas were exposed to the corrodent.

Although such signs of brittle fracture as cleavage steps (Fig. 13) were observed in the dark areas but not in the light, there were still numerous signs of ductility in the dark areas. A dimpled structure was frequently observed, as shown in Fig. 14 . Dimples were also observed frequently in the light areas (Fig. 12b).

The fractographs obtained from the tested tensile specimens revealed approximately what was expected: a predominantly dimpled, transgranular appearance, with the extent of dimpling being smaller in the notched than in the unnotched specimens (Fig. 15 and 16). Occasionally, the fracture was observed to be intergranular (Fig. 15b, 16b, and 17).

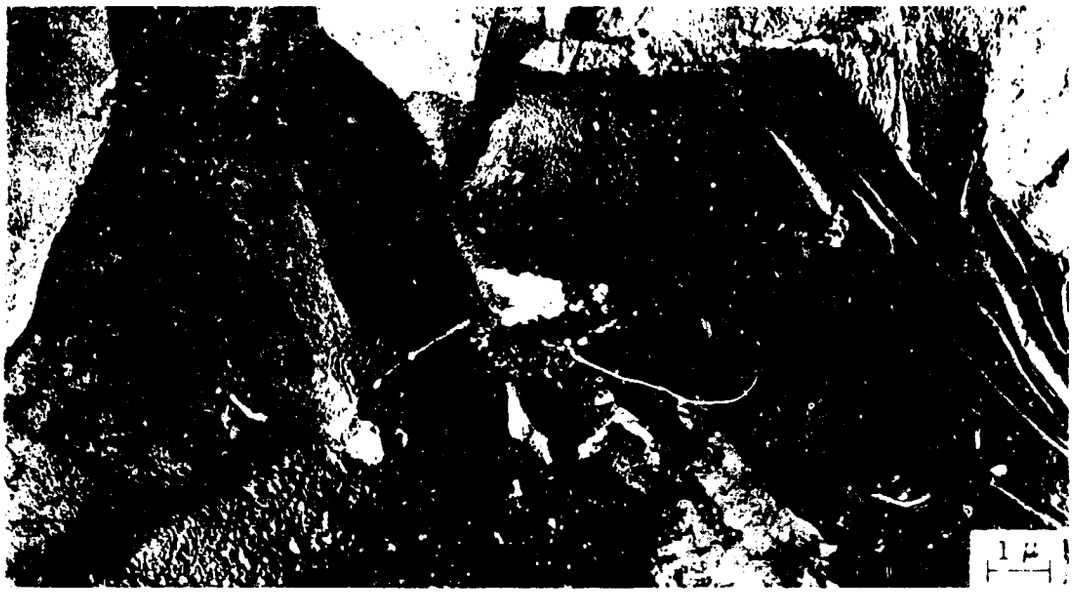

Figure 13. Fractograph of Stress-Corroded Area in a Notched 7075-T73 Specimen Showing Cleavage Steps at A. (Cleavage steps are indicative of brittle fracture.)

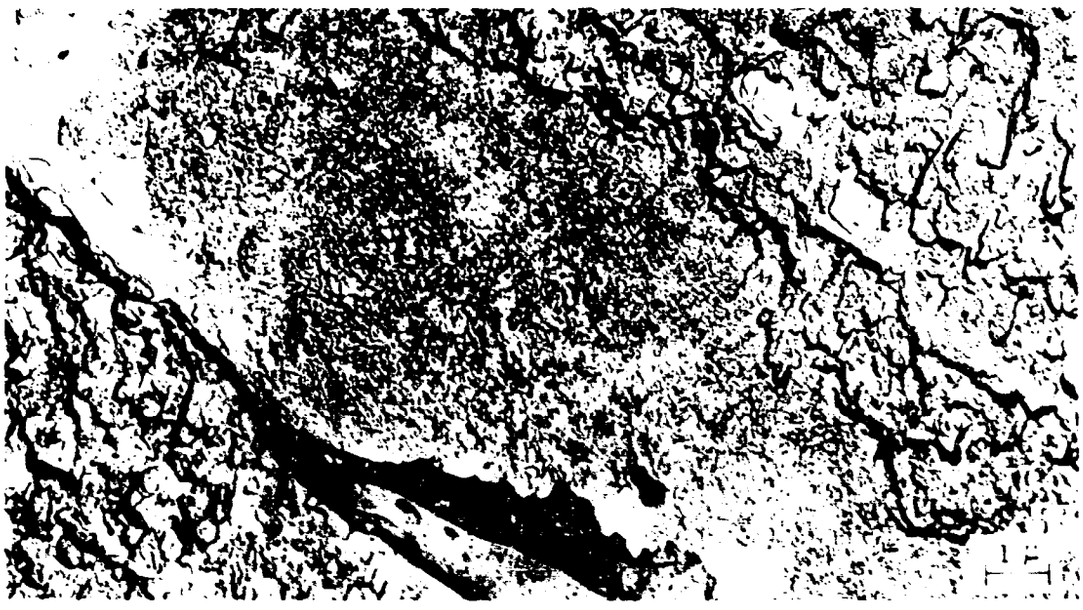

Figure 14. Dimples Indicating Ductility in the Stress-Corroded Area of an Unnotched 7075-T6 Specimen. (Note widespread occurrence of corrosion product.)

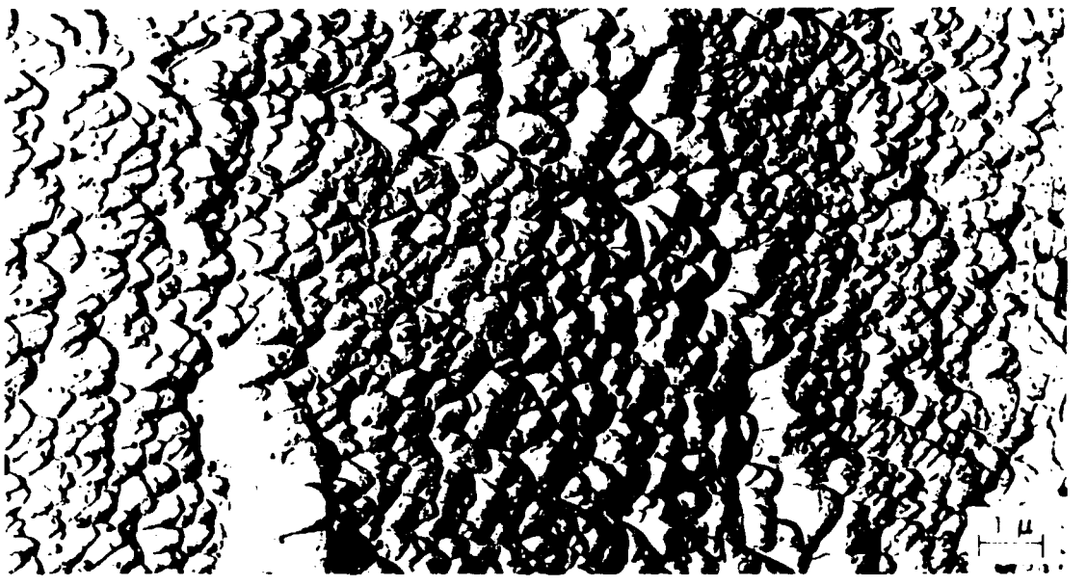

Figure 15a. Transgranular Fracture in an Unnotched 7075-T6 Tensile Specimen Showing Extensive Dimpling

Figure 15b. Fractograph of a Notched 7075-T6 Tensile Specimen Showing Less Extensive Dimpling Than in Unnotched -T6 Specimen

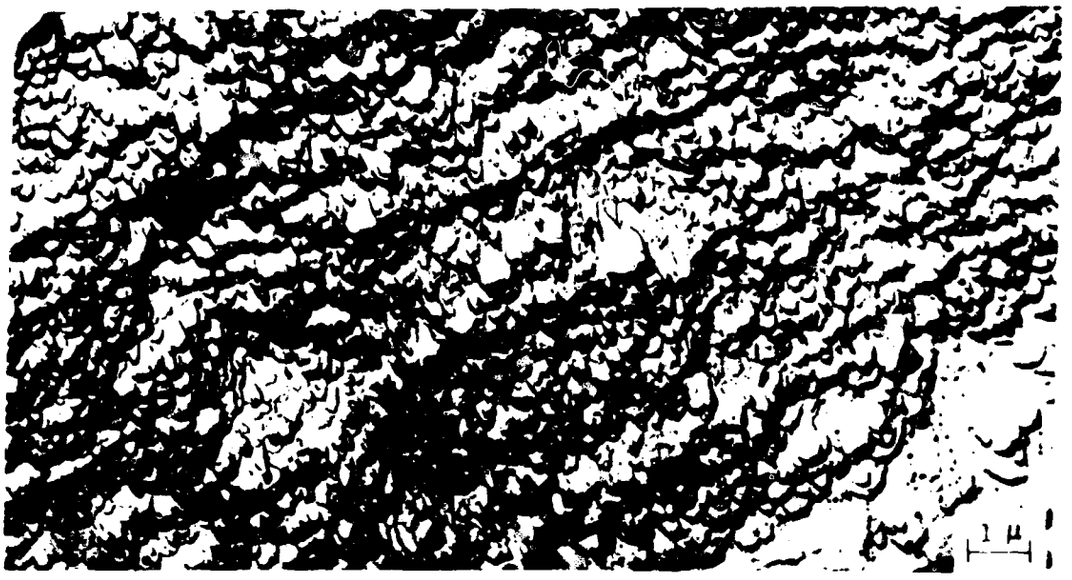

Figure 16a. Transgranular Fracture in an Unnotched 7075-T73 Tensile Specimen Showing Extensive Dimpling

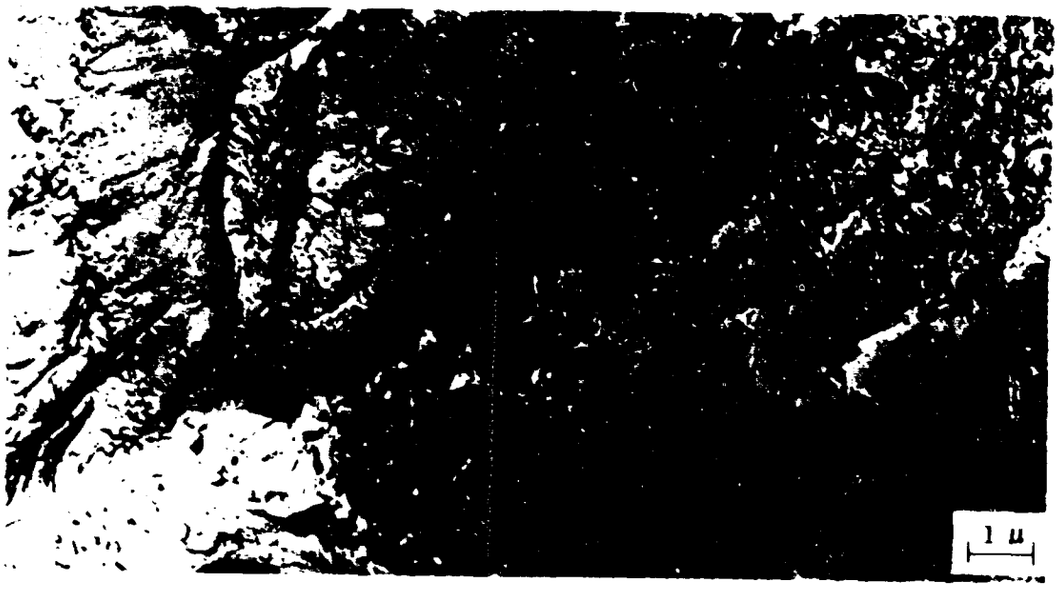

Figure 16b. Fractograph of a Notched 7075-T73 Tensile Specimen Showing Less Extensive Dimpling Than in Unnotched -T73 Specimen

Figure 17. Intergranular Fracture in an Unnotched 7075-T6 Tensile Specimen

SLIP CHARACTERISTICS OF PROGRESSIVELY DEFORMED 7075-T6 AND -T73 SPECIMENS

It was originally planned to supplement the fractographic study of tested stress-corrosion specimens with a slip-line study conducted on a prepolished surface adjacent to the fracture. Considerable difficulty was experienced in attempts to remove the corrosion film without disturbing the underlying slip steps. Numerous laboratory reagents and commercial solutions were utilized including the use of electrochemical techniques. Because of the experimental difficulties, this phase of the program was abandoned in favor of the tensile deformation study described in the following paragraphs. The slip-line study of stress-corrosion specimens may be resumed at a later date when additional background exists on the replication of slip lines in uncorroded samples, and when a stress-corroding medium has been found that does not attack the surface of 7075 alloy as severely as does the 3-1/2 percent NaCl solution.

EXPERIMENTAL PROCEDURE

One series of 7075-T6 and another series of -T73 tensile specimens were deformed in an Instron machine, so the slip characteristics of these tempers could be studied by means of a replica technique. The specimens were of the type shown in Fig. 5. Prior to deformation, they were electropolished according to a procedure described elsewhere (Ref. 1).

The elongation was measured by a deflectometer attached to the moving crosshead of the Instron machine. This quantity varied between 0.020 and 0.045 inch, the latter value being obtained at fracture. The crosshead speed was 0.05 in./min. Typical load-deflection curves for -T6 and -T73 specimens are shown for comparison in Fig. 18. The deformations received by the two sets of specimens were approximately the same and are listed in Table 3.

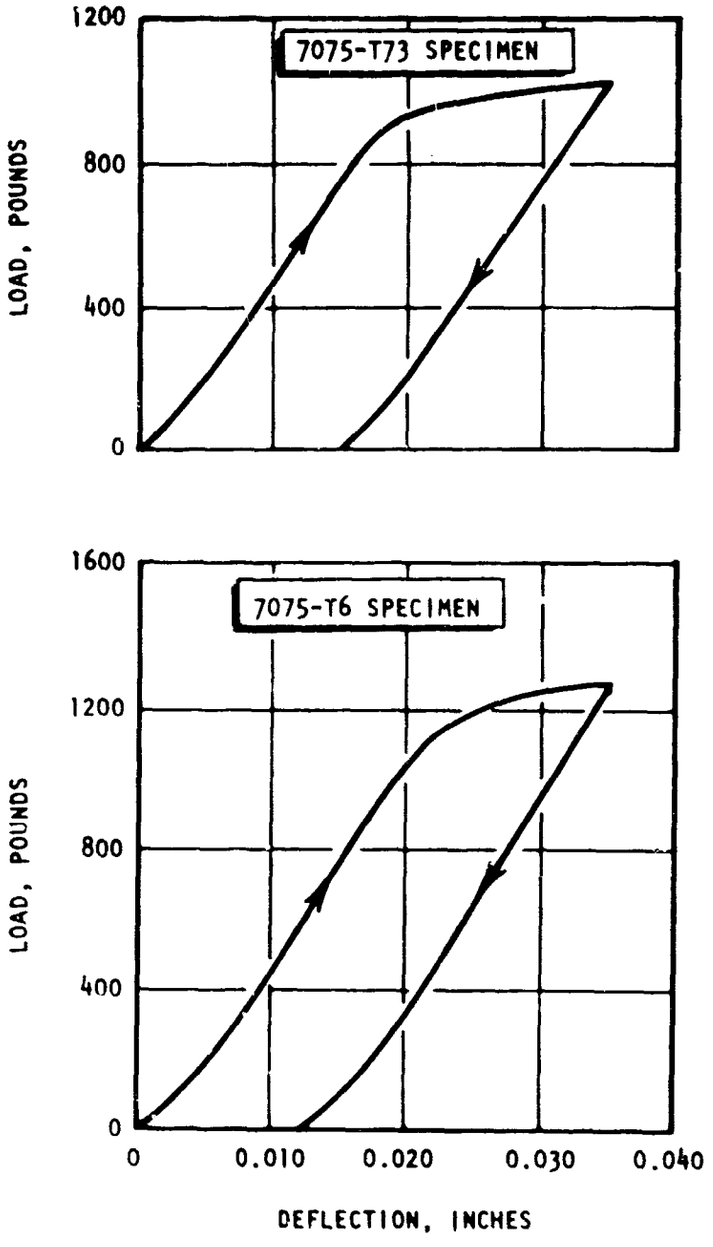

Figure 18. Typical Load vs Deflection Curves for 7075-T6 and -T73 Specimens Deformed in Instron Testing Machine

TABLE 3

ELONGATIONS OF 7075-T6 AND -T73 TENSILE SPECIMENS DEFORMED IN INSTRON MACHINE

Temper	Specimen No.	Elongation, inches
7075-T6	6	0.023
	2	0.025
	3	0.030
	4	0.035
	5	0.040
	1	0.043 (Fracture)
7075-T73	6	0.[illegible]00
	2	0.024
	3	0.030
	4	0.035
	5	0.040
	1	0.046 (Fracture)

A two-stage plastic-carbon replica technique was employed to study the slip lines. The shadowing material was uranium oxide deposited at an angle of 9.5 degrees.

Single-stage techniques offering higher resolution were considered, but these have the disadvantage of requiring a chemical solution for the removal of the replica. Such a solution would very probably entail destruction of the deformed metal surface.

RESULTS AND DISCUSSION

In general, the results obtained for the two series of specimens were similar. The slip lines in -T73 specimens tended to be finer and could not be detected as easily as those in -T6 specimens. This difference may indicate a larger number of active dislocation sources in -T73 than in the -T6 temper, so that in -T6 specimens a given amount of slip would have to be accommodated by a greater displacement on any single slip plane than in -T73 specimens. The slip characteristics of -T6 and -T73 specimens are summarized as follows:

1. The deformation (at a given level of strain) is nonuniform along the length of the specimen from grain to grain, and within a given grain. Most of the deformation does not necessarily occur at the center of the reduced section.
2. Slip is transgranular. There are no indications that initial slip takes place along the grain boundaries.
3. With increasing deformation, slip bands, i.e., clusters of slip lines, appear and cross slip occurs.
4. With increasing deformation, the number of slip lines and bands increases, and the spacing between them decreases.

5. The slip lines and bands tend to become wavy at higher deformations.

Because the deformation was so heterogeneous from grain to grain in a given specimen, a heavily deformed grain could be found in a lightly deformed specimen, and vice versa. This is illustrated in Fig. 19. Hence, the progressive stages in the development of slip lines in -T6 and -T73 specimens, which are portrayed in Fig. 20, do not necessarily correspond with the deformation stages of the specimens themselves.

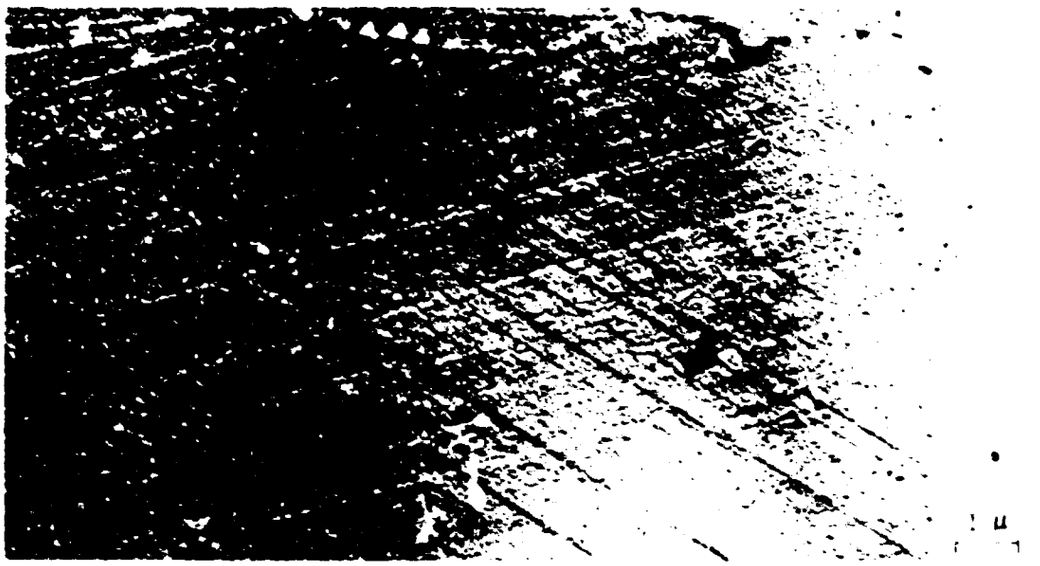

a. Heavily deformed region in a lightly deformed specimen (elongation 0.025 inch)

b. Lightly deformed region in a heavily deformed specimen (elongation 0.040 inch)

Figure 19. Replicas Depicting Heavily and Lightly Deformed Regions in Lightly and Heavily Deformed 7075-T6 Specimens, Respectively

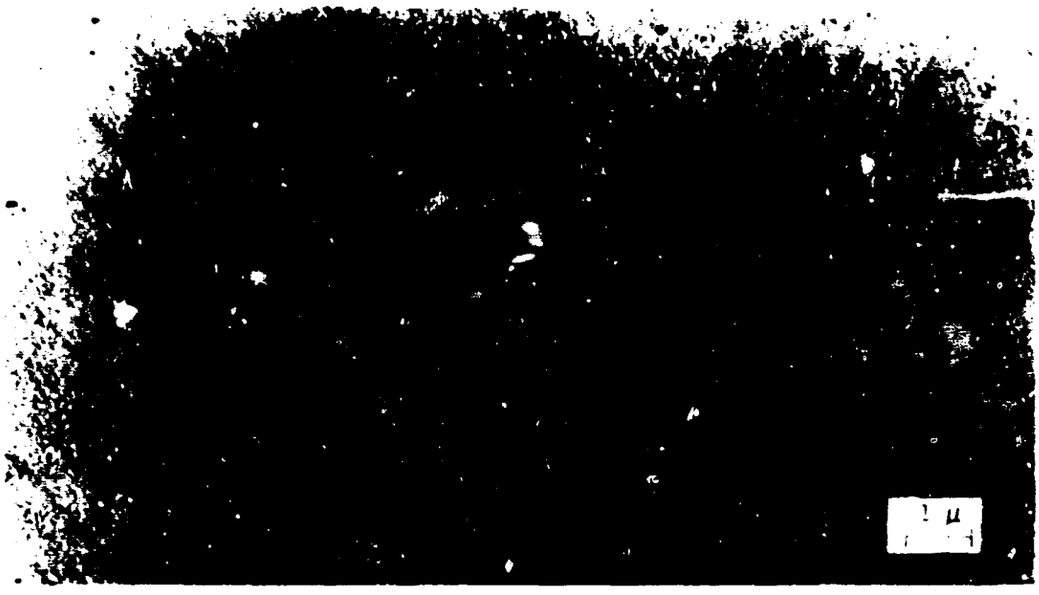

a. 7075-T6 Specimen; Elongation 0.030 Inch (Note widely spaced slip lines and bands at A.)

b. 7075-T6 Specimen; Elongation 0.030 Inch (Note widely spaced slip lines and bands; cross slip at A.)

Figure 20. Progressive Stages in the Development of Slip Lines in 7075 Aluminum

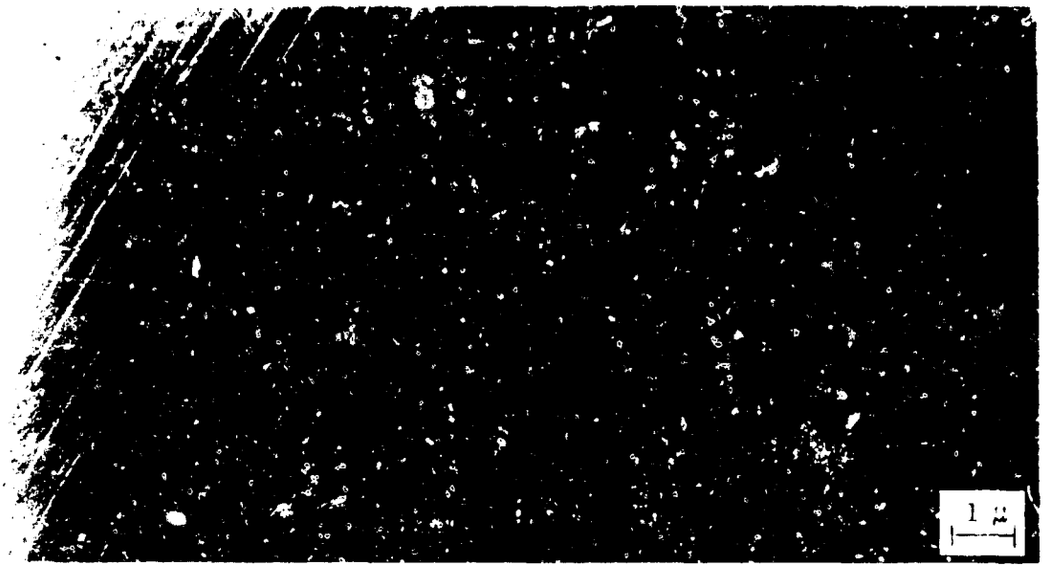

c. 7075-T6 Specimen; Elongation 0.040 Inch (Note closer spacing of slip lines and bands; cross slip at A.)

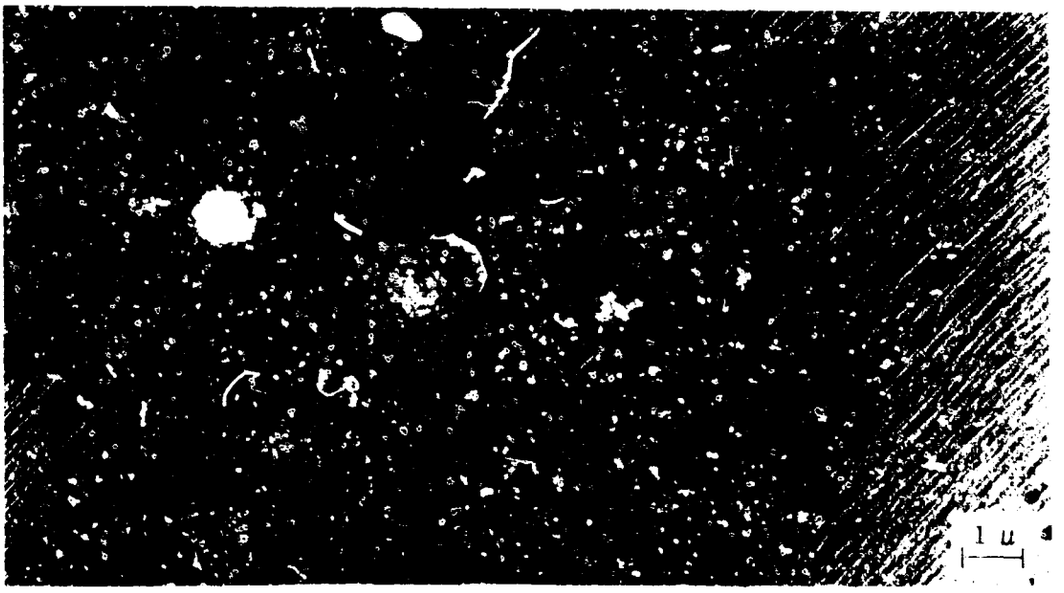

d. 7075-T6 Specimen; Elongation 0.023 Inch (Note very close spacing and fragmentation of slip lines and bands; cross slip at A.)

Figure 20. (Continued)

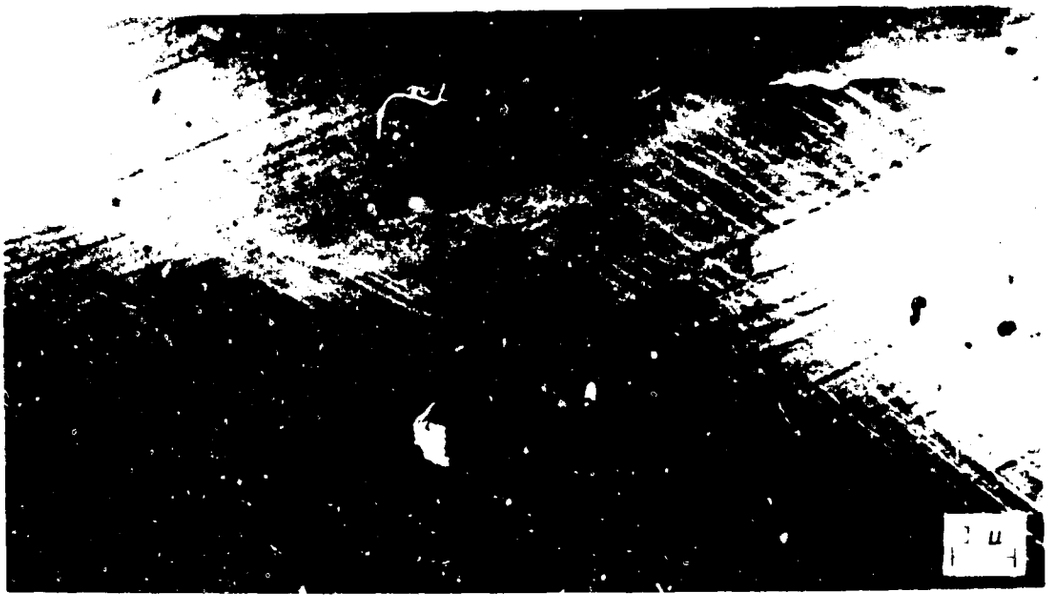

e. 7075-T6 Specimen; Elongation 0.043 Inch (Note fragmentation and waviness of slip lines and bands; large amount of cross slip at A.)

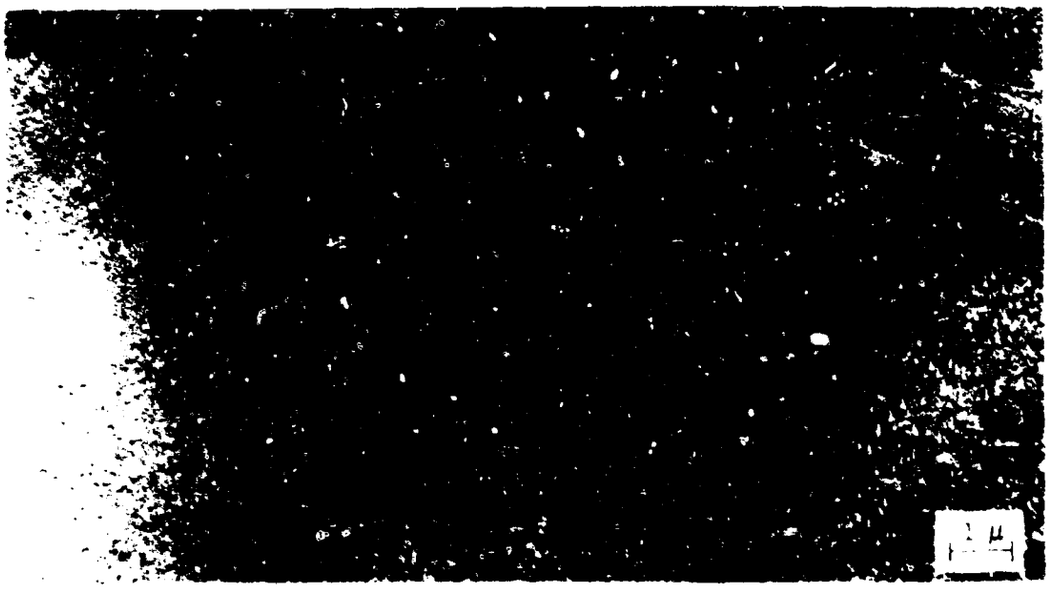

f. 7075-T73 Specimen; Elongation 0.030 Inch (Note widely spaced slip lines and bands at A.)

Figure 20. (Continued)

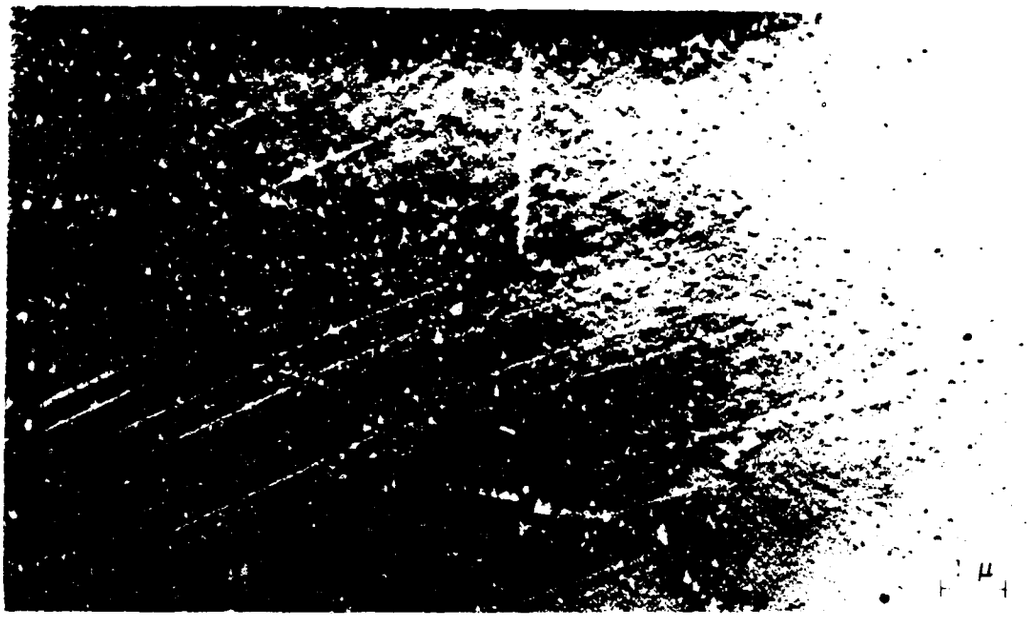

g. 7075-T73 Specimen; Elongation 0.030 Inch (Note closer spacing of slip lines and bands.)

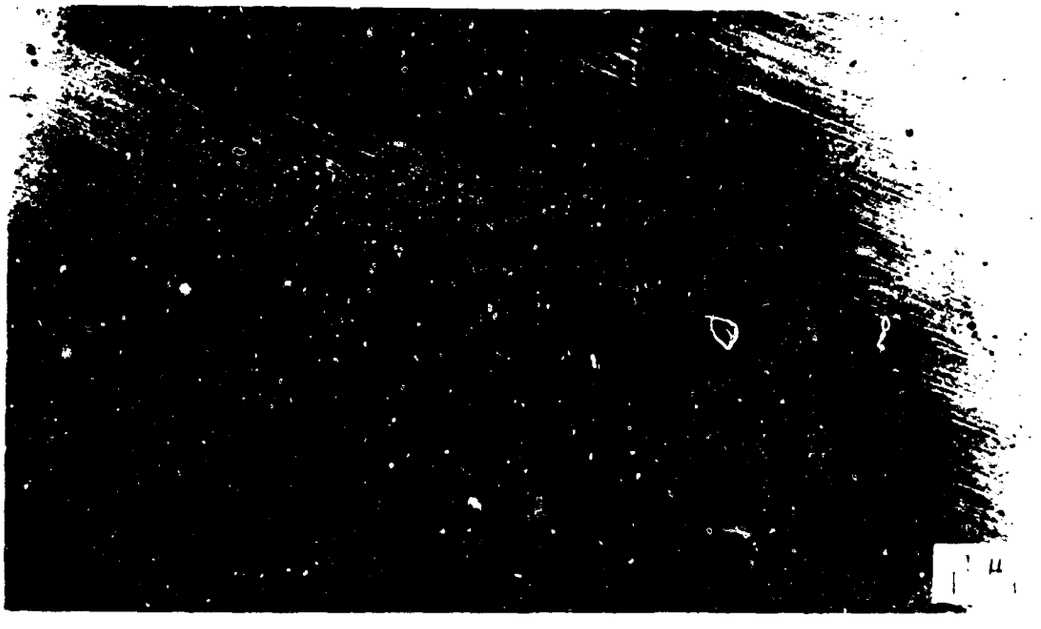

h. 7075-T73 Specimen; Elongation 0.040 Inch (Note very close spacing and fragmentation of slip lines and bands; cross slip at A.)

Figure 20. (Continued)

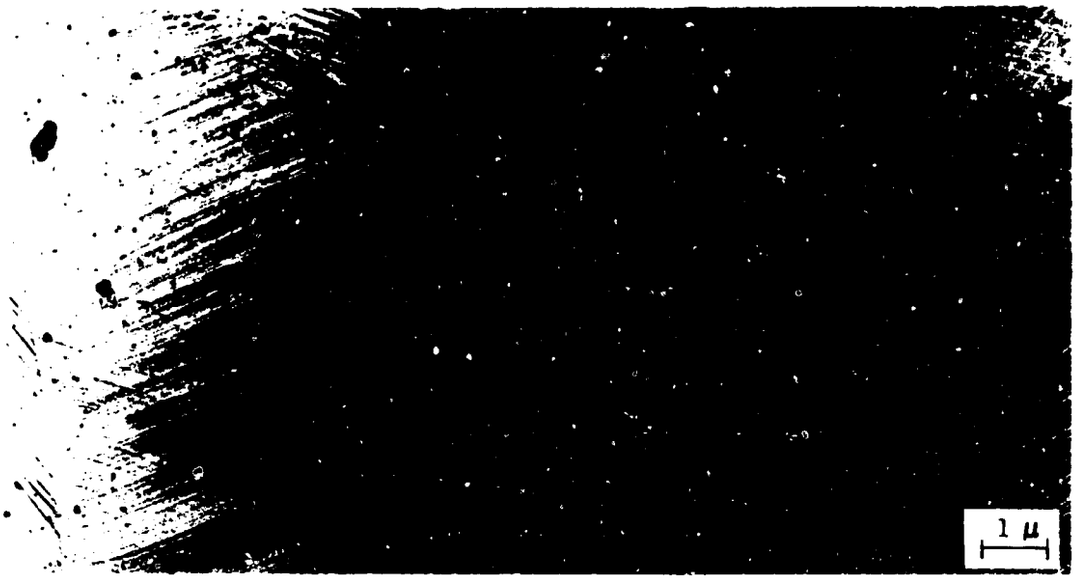

i. 7075-T73 Specime ; Elongation 0.040 Inch (Note large amount of cross slip at A.)

j. 7075-T73 Specimen; Elongation 0.046 Inch (Note extensive waviness and fragmentation of slip lines and bands.)

Figure 20. (Concluded)

AMPLITUDE-DEPENDENT INTERNAL FRICTION MEASUREMENTS

Preliminary amplitude-dependent internal friction measurements were conducted on the 7075 alloy, to obtain information concerning the magnitude of the interaction between the precipitate formed on the dislocation structure and the stress field around the dislocations. Past experiments with irradiated copper (Ref. 9) and with alloys containing small impurity contents (Ref. 10 and 11) have demonstrated that useful information could be obtained.

Four specimens aged to different degrees were tested. These included an underaged (relative to -T6) specimen (6 hours at 250 F), a -T6 specimen, and two overaged (also relative to -T6) specimens (4 hours at 350 F and -T73). Measurements were performed in the 10 to 20 kilocycle range on an elastic constant-internal friction spectrometer, at the North American Aviation Science Center (a detailed description of this apparatus was presented in Ref. 12).

The measurements revealed negligible, if any, difference among the various specimens (Fig. 21). All the specimens demonstrated such sharp dislocation breakaway* at strains of the order of 2×10^{-6} as to suggest that nucleation on the dislocations had proceeded to the point where it swamped the internal friction measurements. A very slight hysteresis in these measurements also was observed, but no aging effects were noted following the breakaway stress experiments that would suggest precipitate motion back to the dislocations (or vice versa).

The conclusions reached from these experiments with the 7075 alloy were that they would be valuable in the future in studying the onset of the aging process of the alloy and that information concerning the kinetics

*The breakaway stress may be defined as the stress at which dislocations tear free of their pinning points, which, in this case, are precipitate particles.

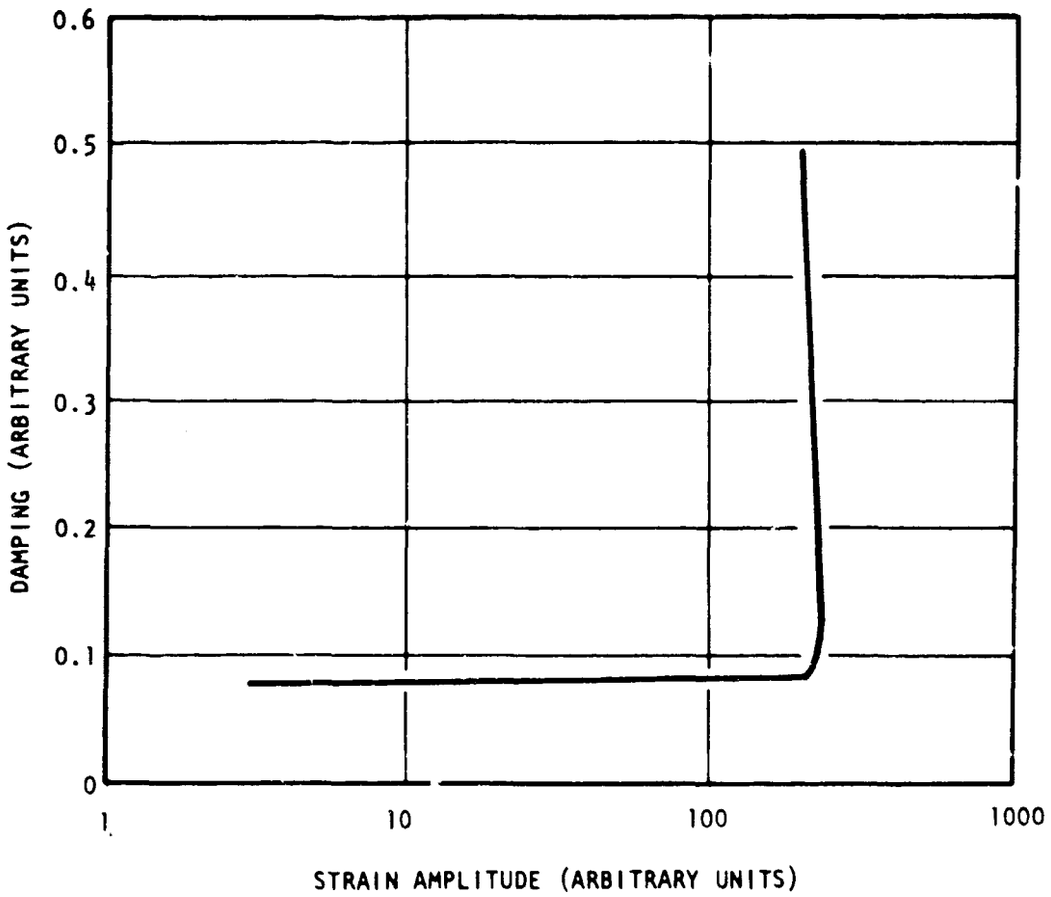

Figure 21. Damping (Internal Friction) vs Strain Amplitude for 7075-T6 Specimen

of precipitate formation could probably be obtained from them. Moreover, it should be possible to obtain information concerning the number of pinning points, the binding energy of the pinning atoms to the dislocations, and the dislocation mobility for the aging domain prior to attaining maximum hardness.

TENTATIVE MECHANISM OF STRESS-CORROSION CRACKING IN 7075 ALUMINUM ALLOY

It nas been shown (Ref. 1) that the two main microstructural differences between the susceptible -T6 and the resistant -T73 tempers of 7075 alloy are: (1) the presence of numerous quenched-in dislocations in -T6 specimens and a negligible (observable) density in -T73 specimens; and (2) a finer precipitate size and a larger number of precipitate particles in -T6 than in -T73 specimens. Both of these differences contribute to the 22 percent greater yield strength of -T6 compared to -T73[1] specimens. A typical thin film micrograph of 7075-T6 alloy is reproduced in Fig. 22.

Thin film microscopy disclosed no differences between the grain boundaries in -T6 and -T73 specimens, other than the close association of dislocations with precipitates in -T6 specimens (Fig. 1) which was not in evidence in -T73 specimens (Ref. 1). The composition of the grain boundary precipitates in the two tempers was shown to be the same, viz., $MgZn_2$, through the use of selected area diffraction and dark field techniques, and the precipitate morphologies and sizes were also similar. A corrosion study of unstressed -T6 and -T73 specimens in an aqueous 3-1 2 percent NaCl solution indicated that the main corrosion process is identical in the two conditions. This process consists of the dissolution of the grain boundary precipitates,[2] which thus act as anodes.

---

(1) Nominal yield and tensile strengths of 7075-T6 alloy are 73,000 and 83,000 psi, respectively. For 7075-T73 alloy these values are 60,000 and 71,000 psi, respectively.

(2) The large $MgZn_2$ particles in the grains also are attacked. However, their dissolution can be discounted in considering the model, because they do not form a continuous path into the metal.

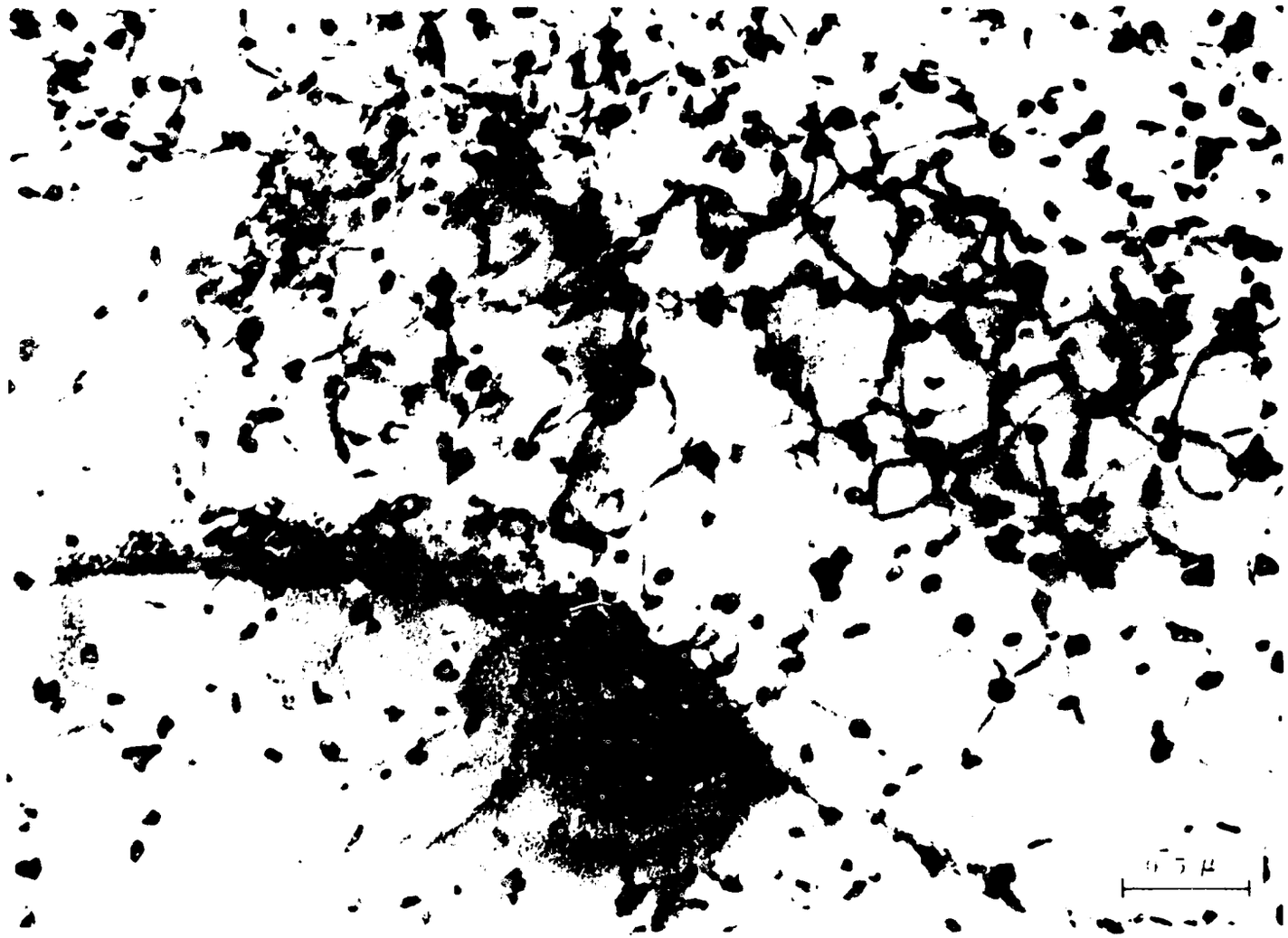

Figure 22. Typical Thin Film Microstructure of 7075-T6 Specimen (Note fine dispersion of GP zones in background, dislocations, and large precipitate particles between which are bowed dislocations)

A schematic drawing of a grain boundary in a 7075-T6 stress-corrosion specimen is shown in Fig. 23 and 24. It will be assumed that this specimen is subjected to a uniaxial tensile stress amounting to 75 percent of yield in the short transverse[1] direction of the original forged billet. A single grain boundary is shown for simplification.

It is proposed that the initiation and propagation of a stress-corrosion crack in 7075 alloy occur as follows (Fig. 23 and 24):

1. An $MgZn_2$ particle present in a grain boundary at the surface is anodic to the aluminum oxide on the surface. Thus it dissolves in the aqueous NaCl solution to form an elliptically shaped pit. (Fig. 23a and 24a). (Pitting is the same in the -T6 and -T73 tempers.)
2. There is a stress concentration at the base of the pit, which falls off rapidly with distance from the pit (Fig. 23a). The stress at the base can be approximated by

$$\sigma_{max} = 2\sigma \left(\frac{c}{r} \right)^{1/2} \qquad (1)$$

where

σ = applied stress (plus any internal contributions)

c = length of the pit

r = radius of curvature at the base (Ref. 13)

In the case of -T6 specimens, a large stress also may act normal to the precipitate-matrix interface shown in Fig. 23a. This stress is a resultant of the applied stress and the dislocation stress field, and as noted in the Calculation of the Dislocation

---

[1] The short transverse direction is the shorter of the two mutually perpendicular directions defining the transverse section of the billet. A tensile stress applied in this direction leads to the most rapid stress-corrosion failure.

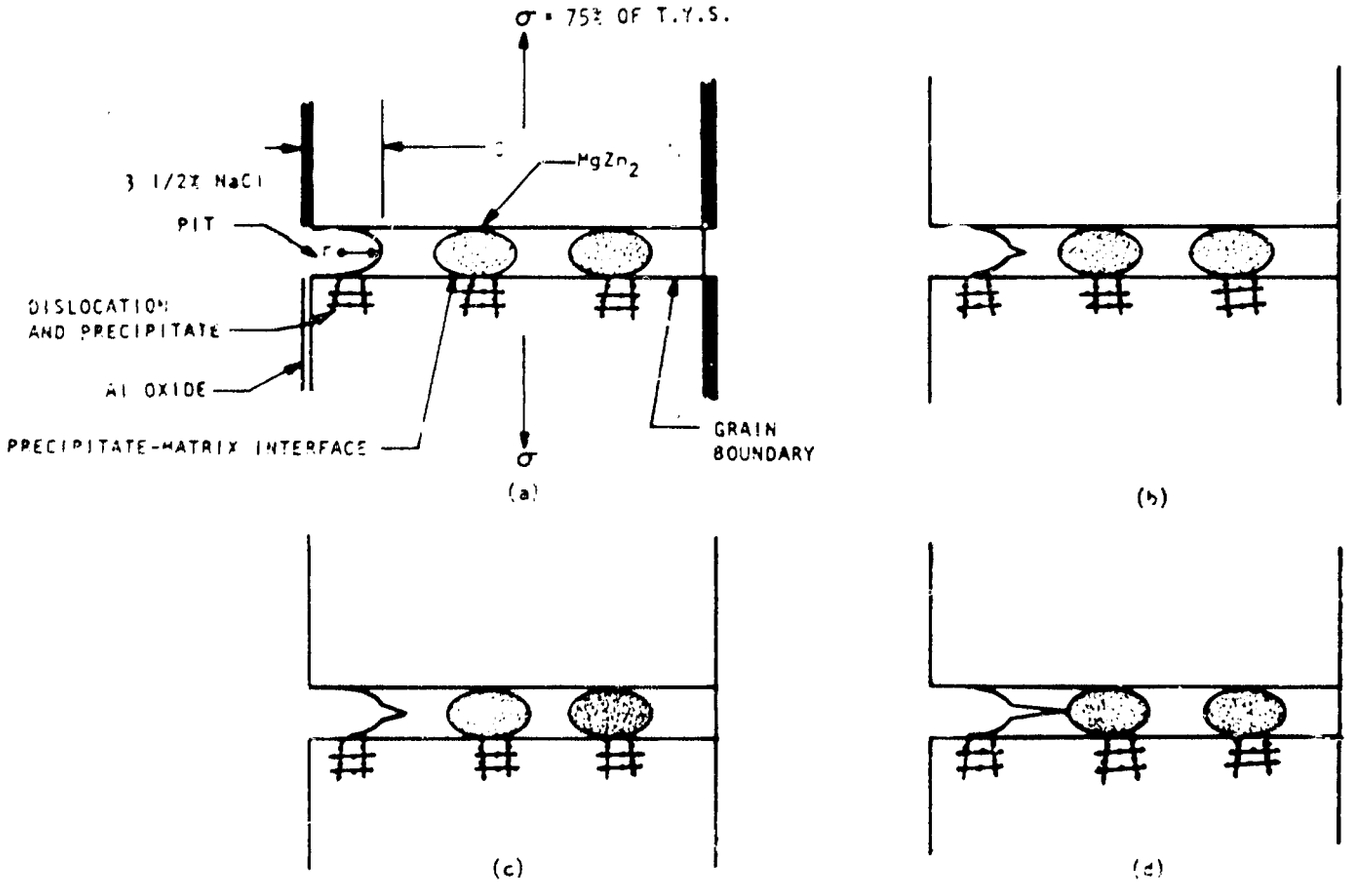

Figure 23. Simplified Schematic Representation of the Stress-Corrosion of 7075-T6 Alloy Loaded to 75 Percent of its Yield Strength (Short-Transverse Orientation)

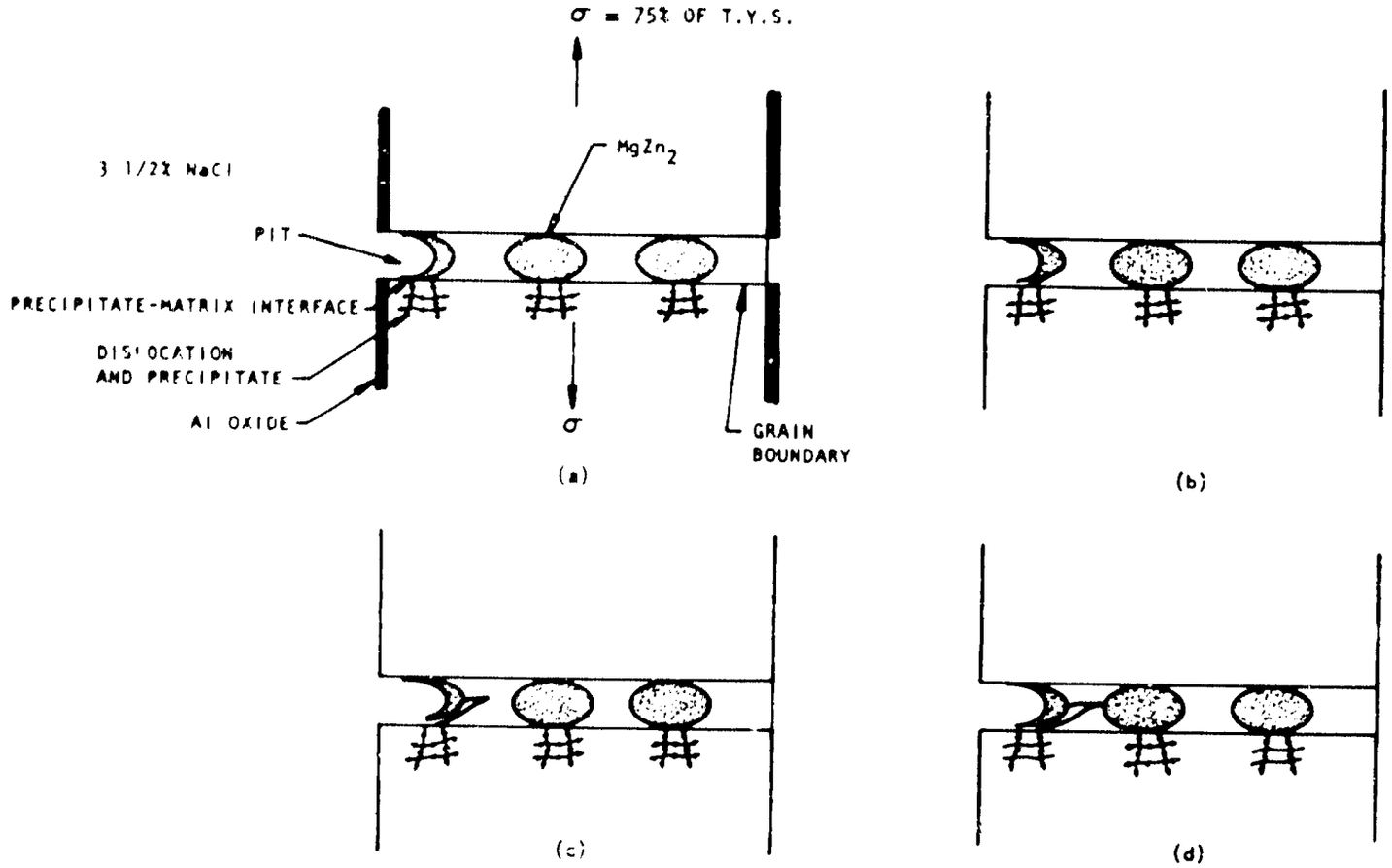

Figure 24. Simplified Schematic Representation of the Stress-Corrosion of 7075-T6 Alloy Loaded to 75 Percent of its Yield Strength (Short-Transverse Orientation)

Stress Field at a Precipitate-Matrix Interface section of this report, it can be very large, theoretically in the order of 250,000 psi. A stress-corrosion crack will thus initiate either at the base of the pit (Fig. 23b) or at the precipitate-matrix interface (Fig. 24b), depending on such factors as maximum tensile stress and the tensile strength of the boundary or precipitate-matrix interface. There is not enough experimental evidence at present to decide where the initiation takes place.

3. In either case (Fig. 23b or 24b), the stress-corrosion crack is observed to be accessible to the corrodent. The assumption is made that the freshly exposed aluminum is anodic to the pitted $MgZn_2$ particle, as well as to the surface oxide of aluminum; thus the initial crack will acquire a configuration in which there is a high stress concentration at the tip (Fig. 23c and 24c). This stress concentration can be reduced by plastic deformation ahead of the crack or by mechanical fracture. Fractographic evidence (presented in the Fractography of Notched and Unnotched 7075-T6 and -T73 Stress-Corrosion and Tensile Specimens section of this report) indicates that both processes can operate in 7075 alloy. Propagation of the crack between particles (Fig. 23d and 24d) will take place by a combination of corrosion and mechanical fracture. The larger the role of slip in reducing the stress concentration at the crack tip, the longer is the corrosion phase of the propagation, and the longer the time to failure (as in -T73 specimens). The larger the role of mechanical fracture, the smaller is the amount of corrosion, and the shorter the time to failure (as in -T6 specimens). If the propagating crack is to grow longer by corrosion, the crack tip must remain film free and thus anodic to the oxide on the walls of the crack. This may be easily visualized where there is at least some dislocation motion ahead of the crack.

4. After the propagating crack has been halted by the next $MgZn_2$ particle, it will become completely covered with oxide, thus transforming the $MgZn_2$ particle into an anode. This particle will now pit, and the cycle comprising Steps 1 to 3 will be repeated.

5. As the total crack length increases, σ_{max} also increases. Finally, when the critical resolved shear stress is exceeded over a critical volume of material, the second state of failure is nucleated. A tensile-type fracture now ensues across the most favorable oriented slip plane(s). Whereas the first stage was predominantly intergranular in nature, the second state is principally transgranular.

DISCUSSION

The consistent results derived from the varied experiments, suggest an important role for mechanical fracture in the propagation of a stress-corrosion crack. However, a crack can also propagate along a grain boundary by corrosion. Both processes can occur in a given condition of the alloy, with one of them predominating. In 7075-T6 alloy, the predominant process is mechanical fracture; in an "off-heat" -T73 alloy, such as the one used for the experiment on notched specimens, or in some susceptible condition intermediate between the -T6 and -T73 tempers, the main process may be corrosion; and in good -T73 specimens it is probably entirely corrosion. Because corrosion is a much slower process than mechanical fracture, the time to failure of 7075-T73 specimens is considerably longer than that of -T6 specimens. Basically, the failure mechanism is believed to be similar in any condition of 7075 alloy; only the proportions of corrosion and mechanical fracture differ.

Whether the stress concentration at the tip of a crack will be relieved by plastic deformation or by mechanical fracture will depend on the ease of activating dislocation sources and the number of these sources. If dislocations can be generated readily, plastic deformation will dominate; otherwise, mechanical fracture will be the principal process. The importance of corrosion as a propagation mode will increase as the extent of plastic deformation increases.

The results of this study have led to a better understanding of the role of dislocations and precipitate particles in the stress-corrosion cracking of 7075 alloy. An increase in the density of either dislocations or particles is now known to increase the susceptibility of this alloy. Such an increase will render dislocation generation and or motion (i.e., plastic flow) more difficult, thus promoting mechanical fracture and rapid stress-corrosion failures.

The important observation has been made (see the Slip Characteristics of Progressively Deformed 7075-T6 and T73 specimen section of this report) that slip lines in 7075-T6 specimens traverse a given grain rather freely, instead of being concentrated in narrow regions surrounding the grain boundaries. This finding is contrary to what has been found in analogous British alloys based on the Al-Zn-Mg system (e.g., D.T.D. 687, Ref. 14). Experience with the latter alloys has shown that after aging to maximum hardness, slip lines were confined to the precipitate-free (denuded), grain boundary regions. Intergranular failures with elongations as high as 12 percent could be obtained under such conditions.

Certain investigators have inferred from the tensile results on the British alloys that stress-corrosion cracking in these alloys occurs as a result of preferential plastic flow in the denuded zones, followed by preferential corrosive attack along these zones. Such an inference cannot be made in the case of 7075-T6 specimens, where a normal tensile failure features transgranular slip (Fig. 20) and transgranular cracking. Furthermore, denuded zones have been observed only infrequently in 7075-T6 specimens. It could be reasonably assumed that whatever zones were present would be preferentially cold-worked upon the application of explosive shock loading or tensile deformation, thus negating their possible role in stress corrosion. However, the opposite has been observed; cold working decreased the resistance to stress corrosion.

Some of the most direct evidence against a denuded zone theory for alloys based on Al-Zn-Mg was obtained recently by Holl (Ref. 15). Holl, studying an Al alloy containing 5.7 percent Zn-2.7 percent Mg-0.5 percent Cu-($\leq$ 0.3 percent Si + Fe), found that two susceptible conditions were free of denuded zones, while two resistant conditions did show denuded zones. The overall distribution and nature of precipitates within the matrix were concluded to determine stress-corrosion susceptibility through their control over deformation behavior.

The high sensitivity of stress-corrosion resistance to particle density raises the possibility that a correlation can be found between one of the age-hardening parameters and stress-corrosion lifetime. Various functions of the interparticle spacing or volume fraction of precipitate, which have been used to predict macroscopic yield strength, are suggested for initial trial, because a rough correlation appears to exist between the yield strength and stress-corrosion time to failure of shock loaded 7075 alloy. The quantitative forecast of stress-corrosion resistance from a simple microstructural examination of 7075 alloy is an interesting prospect. Similar forecasts may be possible for other precipitation-hardening systems as well.

CONCLUSIONS

The following conclusions have been reached based upon the present investigation:

1. Calculation of the stress field around an edge dislocation neighboring a grain boundary precipitate indicates that the tensile stress which acts normal to the precipitate-matrix interface can be very large theoretically (precluding plastic flow), in the order of 250,000 psi. Stress-corrosion cracks in 7075-T6 specimens may initiate at this interface or at the base of a pit.

2. The stress-corrosion resistance of 7075 aluminum is lowered more by an increase in precipitate-particle density than by an increase in dislocation density.

3. The basic difference between a susceptible temper such as -T6 and a resistant temper such as -T73 resides in their respective capacities for plastic deformation at the tip of a crevice. The -T6 temper is limited in its ability to deform, primarily because of its high density of GP zones, while the -T73 temper can deform more easily because of its lower density of precipitate particles. A high stress concentration in the -T6 temper is more likely to be relieved by mechanical fracture than plastic flow, whereas in -T73 specimens plastic flow is a more likely mechanism.

4. A rapid, intergranular stress-corrosion failure can be induced in a 7075-T73 specimen through the introduction of a notch. With its capacity for plastic flow thus limited, -T73 specimens behave in a manner similar to -T6 specimens.

5. A stress-corrosion failure in 7075-T6 specimens (or in notched -T73) involves at least some plastic flow, as evidenced by the dimpling observed in fractographs.

6. The slip characteristics of 7075-T6 and -T73 specimens are generally similar. Slip is transgranular and there are no indications that initial slip takes place along the grain boundaries.

With increasing deformation, slip bands, i.e., clusters of slip lines, appear, and cross slip occurs.

7. The effect of increasing stress is to prolong the time to failure of unnotched 7075-T73 stress-corrosion specimens.

FUTURE WORK

The results of the experiments reported herein and of others conducted previously have suggested a number of additional investigations. The experiments that are planned for the immediate future will be designed primarily to provide a greater degree of quantitative corroboration of the present theory. This can be accomplished by correlating (1) a parameter reflecting dislocation mobility, such as internal friction or stress relaxation, and (2) a microstructural parameter such as particle density or spacing, with stress-corrosion susceptibility. Another objective of future effort will be to determine from thin film examination whether dislocations in 7075-T6 specimens posses the appropriate geometry with respect to grain boundary particles to cause high tensile stresses at the particle matrix interface. Also planned are a qualitative study of slip at the tip of a propagating crack, using replica techniques, and an initiation of studies aimed at optimizing the combination of yield strength and stress-corrosion resistance in the 7075 alloy. The application of the fundamental understanding of the mechanism of stress-corrosion cracking, which is being developed, to such an optimization of properties, remains the ultimate goal of this work. It has been demonstrated during a previous program (Ref. 2) that the optimum combination of properties for 7075 alloy is obtained by cold working a condition that is sufficiently overaged to ensure that there is no further precipitation. In shock loading experiments, the minimum overaging time required at 350 F for a t_f in excess of 30 days was 3 hours, and the yield strength accompanying this t_f was ~68,000 psi. There appears to be no reason why conventional deformation processes, such as rolling and forging, could not give the same results as explosive shocking, providing the particular overaging time required in each case is first determined. It was also demonstrated during a tensile deformation experiment on -T73 specimens that the introduction of dislocations had no discernible effect on t_f. Shock loading, perhaps because of the higher dislocation densities introduced, had a slightly deleterious effect on t_f (decreasing from 51 to 40 days); the yield strength was raised at the same time, however, to approximately 70,000 psi. Future effort in this area of investigation will incorporate the preceding findings and will concentrate on conventional methods of deformation that can be easily applied in conjunction with heat treatment.

days); the yield strength was raised at the same time, however, to approximately 70,000 psi. Future effort in this area of investigation will incorporate the preceding findings and will concentrate on conventional methods of deformation that can be easily applied in conjunction with heat treatment.

REFERENCES

1. Jacobs, A. J., "The Role of Dislocations in the Stress-Corrosion Cracking of 7075 Aluminum Alloy," ASM Trans. Quarterly, 58, 579 (1965).

2. Jacobs, A. J., "A New Model for Stress-Corrosion Cracking in the 7075 Aluminum Alloy," Paper presented at the 1966 National Metal Congress, Metal Science Forum on Stress Corrosion, Chicago, Illinois, 1 November 1966.

3. McHardy, J., "Investigation of the Mechanism of Stress Corrosion of Aluminum Alloys," Bureau of Naval Weapons, Contract NOw 64-0170-c, Final Report, 16 February 1965 to 16 February 1966.

4. Dundurs, J., and T. Mura, J. Mech. Phys. Solids, 12, 177, (1964).

5. Gensamer, M., Strength of Metals Under Combined Stresses, p. 22 American Society for Metals, Cleveland, Ohio (1941).

6. Sprowls, D. O., and R. H. Brown, Technical Paper No. 17, Aluminum Company of America, Pittsburgh, Penssylvania (1962).

7. Farmery, H. K., and U. R. Evans, J. Inst. Metals, 84, 413 (1955-56).

8. Colner, W. H., and H. T. Francis, J. Electrochem. Soc., 105, 377 (1958).

9. Thompson, D. O., and V. K. Pare, "Use of Anelasticity in Investigating Radiation Damage and the Diffusion of Point Defects," Physical Acoustics, Vol. IIIA, Academic Press, Inc., New York, 1966, ed. by W. P. Mason, Chapter 7.

10. Beshers, D. N., J. Appl. Phys., 30, 2, 252 (1959).

11. Fiore, N. F., and C. L. Bauer, J. Appl. Phys., 35, 2242 (1964).

12. Thompson, D. O. and F. M. Glass, Rev. Sci. Inst., 29, 11, 1034 (1958).

13. Inglis, C. E., Trans. Inst. Naval Architects, 55, 219, (1913).

14. Thomas, G. and J. Nutting, "The Aging Characteristics of Aluminum Alloys: Electron Microscope Studies of Alloys Based on the Aluminum-Zinc-Magnesium System," J. Inst. Metals, 88, 81, (1956-60).

15. Holl, H. A., "Deformation Substructure and Susceptibility to Intergranular Stress Corrosion Cracking in an Aluminum Alloy," to be published in Corrosion.

UNCLASSIFIED

Security Classification

DOCUMENT CONTROL DATA - R&D

(Security classification of title, body of abstract and indexing annotation must be entered when the overall report is classified)

1. ORIGINATING ACTIVITY (Corporate author) Rocketdyne, a Division of North American Aviation, Inc., 6633 Canoga Avenue, Canoga Park, California	2a. REPORT SECURITY CLASSIFICATION UNCLASSIFIED 2b. GROUP

3. REPORT TITLE

STUDY OF STRESS-CORROSION CRACKING OF ALLUMINUM ALLOYS

4. DESCRIPTIVE NOTES (Type of report and inclusive dates)

Final Report (6 April 1966 through 5 April 1967)

5. AUTHOR(S) (Last name, first name, initial)

Jacobs, A. J.

6. REPORT DATE	7a. TOTAL NO. OF PAGES	7b. NO. OF REFS
5 May 1967		

8a. CONTRACT OR GRANT NO.	9a. ORIGINATOR'S REPORT NUMBER(S)
NOw 66-0309d b. PROJECT NO.	R-7026
c.	9b. OTHER REPORT NO(S) (Any other numbers that may be assigned this report)
d.	

10. AVAILABILITY/LIMITATION NOTICES

11. SUPPLEMENTARY NOTES	12. SPONSORING MILITARY ACTIVITY
	Naval Air Systems Command Department of the Navy Washington, D.C.

13. ABSTRACT A further clarification of the mechanism of stress-corrosion cracking in 7075 aluminum alloy was obtained, particularly with regard to the role of dislocations in the mechanism and to the relationship between dislocation mobility and susceptibility to stress-corrosion cracking; high dislocation mobility reduces susceptibility. It was demonstrated during stress-corrosion tests on 7075-T73 specimens that had undergone prior plastic deformation, that the introduction of dislocations along did now lower the dislocation mobility sufficiently to diminsh the stress-corrosion resistance. This is in contrast to similar experiments with -T6 specimens, wherein precipitation was induced by similiar deformation and the mobility was reduced sufficiently to lower the stress-corrosion resistance. An important role for immobilized dislocations was also suggedted by a theoretical calculation of the stress field around an edge dislocation which neighbors a grain boundary precipitate. This calculation, which was based only on elasticity theory and thus precluded plastic flow, indicated that a large tensile stress, theoretically as high as 250,000 psi, could act normal to the precipitate-matrix interface. When the capacity for plastic flow (i.e., the dislocation mobility) was intentionally reduced by notching a stress-corrosion specimen, a rapid failure could be induced in normally resistant 7075-T73 alloy. Fractographic analysis revealed that this was a true intergranular, stress-corrosion failure, similar in every respect to a stress-corrosion failure in 7075-T6 alloy. A slip-line study of progressively deformed 7075-T6 and -T73 alloys indicated that slip takes place throughout the grain and is not confined

DD FORM 1 JAN 64 1473

UNCLASSIFIED

Security Classification

14 KEY WORDS	LINK A		LINK B		LINK C	
	ROLE	WT	ROLE	WT	ROLE	WT
Aluminum Alloys Stress-Corrosion Cracking Plastic Deformation Dislocations Grain Boundaries Fractographic Analysis						

INSTRUCTIONS

1. **ORIGINATING ACTIVITY:** Enter the name and address of the contractor, subcontractor, grantee, Department of Defense activity or other organization *(corporate author)* issuing the report.

2a. **REPORT SECURITY CLASSIFICATION:** Enter the overall security classification of the report. Indicate whether "Restricted Data" is included. Marking is to be in accordance with appropriate security regulations.

2b. **GROUP:** Automatic downgrading is specified in DoD Directive 5200.10 and Armed Forces Industrial Manual. Enter the group number. Also, when applicable, show that optional markings have been used for Group 3 and Group 4 as authorized.

3. **REPORT TITLE:** Enter the complete report title in all capital letters. Titles in all cases should be unclassified. If a meaningful title cannot be selected without classification, show title classification in all capitals in parenthesis immediately following the title.

4. **DESCRIPTIVE NOTES:** If appropriate, enter the type of report, e.g., interim, progress, summary, annual, or final. Give the inclusive dates when a specific reporting period is covered.

5. **AUTHOR(S):** Enter the name(s) of author(s) as shown on or in the report. Enter last name, first name, middle initial. If military, show rank and branch of service. The name of the principal author is an absolute minimum requirement.

6. **REPORT DATE:** Enter the date of the report as day, month, year; or month, year. If more than one date appears on the report, use date of publication.

7a. **TOTAL NUMBER OF PAGES:** The total page count should follow normal pagination procedures, i.e., enter the number of pages containing information.

7b. **NUMBER OF REFERENCES:** Enter the total number of references cited in the report.

8a. **CONTRACT OR GRANT NUMBER:** If appropriate, enter the applicable number of the contract or grant under which the report was written.

8b, 8c, & 8d. **PROJECT NUMBER:** Enter the appropriate military department identification, such as project number, subproject number, system numbers, task number, etc.

9a. **ORIGINATOR'S REPORT NUMBER(S):** Enter the official report number by which the document will be identified and controlled by the originating activity. This number must be unique to this report.

9b. **OTHER REPORT NUMBER(S):** If the report has been assigned any other report numbers *(either by the originator or by the sponsor)*, also enter this number(s).

10. **AVAILABILITY/LIMITATION NOTICES:** Enter any limitations on further dissemination of the report, other than those imposed by security classification, using standard statements such as:

(1) "Qualified requesters may obtain copies of this report from DDC."

(2) "Foreign announcement and dissemination of this report by DDC is not authorized."

(3) "U. S. Government agencies may obtain copies of this report directly from DDC. Other qualified DDC users shall request through _____."

(4) "U. S. military agencies may obtain copies of this report directly from DDC. Other qualified users shall request through _____."

(5) "All distribution of this report is controlled. Qualified DDC users shall request through _____."

If the report has been furnished to the Office of Technical Services, Department of Commerce, for sale to the public, indicate this fact and enter the price, if known.

11. **SUPPLEMENTARY NOTES:** Use for additional explanatory notes.

12. **SPONSORING MILITARY ACTIVITY:** Enter the name of the departmental project office or laboratory sponsoring *(paying for)* the research and development. Include address.

13. **ABSTRACT:** Enter an abstract giving a brief and factual summary of the document indicative of the report, even though it may also appear elsewhere in the body of the technical report. If additional space is required, a continuation sheet shall be attached.

It is highly desirable that the abstract of classified reports be unclassified. Each paragraph of the abstract shall end with an indication of the military security classification of the information in the paragraph, represented as *(TS), (S), (C), or (U)*.

There is no limitation on the length of the abstract. However, the suggested length is from 150 to 225 words.

14. **KEY WORDS:** Key words are technically meaningful terms or short phrases that characterize a report and may be used as index entries for cataloging the report. Key words must be selected so that no security classification is required. Identifiers, such as equipment model designation, trade name, military project code name, geographic location, may be used as key words but will be followed by an indication of technical context. The assignment of links, rules, and weights is optional.